JOURNAL OF COMPUTATIONAL PHYSICS 103, 189–221 (1992)

INVITED PAPER

Ensuring Well-Posedness by Analogy; Stokes Problem and Boundary Control for the Wave Equation

R. GLOWINSKI

Department of Mathematics, University of Houston, Houston, Texas 77204-3476 and Université Paris VI and CERFACS, France

Received August 6, 1991; revised June 4, 1992

DEDICATED TO H. O. KREISS ON HIS 60TH BIRTHDAY

In this article we give a comparative discussion of the finite element approximation of two partial differential equation problems. These two problems which are apparantly quite unrelated are the Stokes problem for incompressible viscous flow and an exact boundary controllability problem for the wave equation. We show that straightforward discrete approximations to these problems yield approximate problems which are ill-posed. The analysis of the ill-posedness of the above problems shows an identical cause, namely the strong damping of the high frequency modes, beyond a critical wave number. From this analogy, a well-known cure for the discrete Stokes problem, i.e., using more accurate approximations for velocity than for pressure, provides a simple way to eliminate the ill-posedness of the discrete exact boundary controllability problem. Numerical examples concerning the control problem testify about the soundness of the new approach. To conclude this paper one takes advantage of the previous analysis to give a brief discussion of the wavelet approximation of the Stokes problem, for Dirichlet boundary conditions.

1. HISTORICAL PERSPECTIVE: MOTIVATION AND SYNOPSIS

Motivated by the *wavelet approximation* of the *Stokes problem*, with *Dirichlet boundary conditions* on the velocity, we recently undertook (in [1]) an analysis of the *ill-posedness* of the discrete Stokes problems when *similar finite element approximations and identical meshes are used for both velocity and pressure*. From that analysis, it appears that the ill-posedness of the above discrete Stokes problem is due to the *strong damping* of the *high frequency* pressure modes, *beyond a critical wave number*. Indeed, the above analysis strongly supports the well-known cure of the discrete Stokes problem consisting of using qualitatively similar finite element approximations for pressure and velocity, the pressure one being associated to a mesh *twice coarser* than the velocity mesh (other cures are possible as shown in, e.g., [2]).

Considering now the exact boundary controllability problem whose numerical solution is addressed in [3, 4], it follows from J. L. Lions [5–7] that it can be reduced to a *functional equation* whose solution gives the initial data of an adjoint wave equation, whose solution will provide in turn the exact control we are looking for (this approach is fully described in Section 3). The above functional equation is associated to an operator which has essentially the same properties as the operator that one obtains if one eliminates the velocity in the Stokes equations (see Section 2 for details); indeed in [4] we have used this similarity since we have shown there that both problems can be solved by a general *conjugate gradient algorithm*, well suited to *linear functional equations* in Hilbert spaces for *strongly elliptic* and *self-adjoint* operators. Actually, the similarity between both problems goes beyond the above structural analogy, since a straightforward (finite element in space/finite difference in time) discretization of the boundary control problem yields an ill-conditioned discrete operator $\bigwedge_h^{\Delta t}$ whose *damping properties* are *exactly* the same than those of the discrete Stokes operator (if one uses similar finite element approximations and identical meshes for pressure and velocity). This analogy clearly suggests that the spirit of the cure which works for the Stokes problem (i.e., using a pressure mesh twice coarser than the velocity one) may also provide a way to eliminate the ill-posedness of the discrete boundary control problem. This prediction seems to be true as we shall see in Section 4.

The content of this article is the following: In Section 2 we discuss the finite element approximation of the Stokes problem for Dirichlet boundary conditions on the velocity. In Section 3, we discuss the solution of an exact boundary controllability problem for the wave equation, by the J. L. Lions *Hilbert uniqueness method* (HUM) (see [3–7]); we show in particular that classical finite element in space/finite

0021-9991/92 $5.00

difference in time implementations of HUM yield discrete problems which are ill-posed. We also show that the cure used for the discrete Stokes problem provides a discrete boundary control problem, which on the basis of the numerical experiments of Section 4, is well-posed, *uniformly* in h and Δt, and gives optimal orders of convergence (the *conjugate gradient* solution of the discrete boundary control problem is fully described in Section 3). In Section 5, we briefly discuss the application of the concepts of Section 2 to the *wavelet solution* of the Stokes problem for Dirichlet boundary conditions on the velocity. Finally, in an appendix we discuss the solution of the Stokes problem of Section 2 as an application of a fairly general conjugate gradient algorithm described in Section 3.5.

2. THE STOKES PROBLEM AND ITS FINITE ELEMENT APPROXIMATIONS

2.1. Formulation of the Stokes Problem

Let Ω be a *bounded domain* of $\mathbb{R}^d$ ($d=2, 3$ in practice) and let Γ denote its boundary; we suppose that Γ (and therefore Ω) is invariant with time. We suppose next that an *incompressible* (very) *viscous flow* is taking place in Ω modelled by the following unsteady Stokes equations

$$\frac{\partial \mathbf{u}}{\partial t} - \nu \nabla^2 \mathbf{u} + \nabla p = \mathbf{f} \qquad \text{in } \Omega, \tag{2.1}$$

$$\nabla \cdot \mathbf{u} = 0 \qquad \text{in } \Omega, \tag{2.2}$$

$$\mathbf{u} = \mathbf{g} \qquad \text{on } \Gamma, \tag{2.3}$$

$$\mathbf{u}(x, 0) = \mathbf{u}_0(x), \qquad x \in \Omega. \tag{2.4}$$

In (2.1)–(2.4):

(a) $\mathbf{u} = \{u_i\}_{i=1}^d$ is the *velocity*, p is the *pressure*,

(b) $x = \{x_i\}_{i=1}^d$, $\nabla = \{\partial/\partial x_i\}_{i=1}^d$, $\nabla^2 = \Delta = \sum_{i=1}^d \partial^2/\partial x_i^2$, $\nabla \cdot \mathbf{u} = \sum_{i=1}^d \partial u_i/\partial x_i$,

(c) $\nu(>0)$ is a *viscosity coefficient*, $\mathbf{f}$ is a *density of external forces*,

(d) $\nabla \cdot \mathbf{u} = 0$ is the *incompressibility condition*; it implies

$$\int_\Gamma \mathbf{g} \cdot \mathbf{n} \, d\Gamma = 0, \tag{2.5}$$

where $\mathbf{n}$ is the outward unit normal vector at Γ, and also

$$\nabla \cdot \mathbf{u}_0 = 0 \qquad \text{in } \Omega, \tag{2.6}$$

$$\mathbf{u}_0 \cdot \mathbf{n} = \mathbf{g} \cdot \mathbf{n} \qquad \text{on } \Gamma, \text{ at } t = 0 \tag{2.7}$$

(in (2.5)–(2.7), $\mathbf{y} \cdot \mathbf{z}$ is the canonical scalar product of $\mathbb{R}^d$, i.e., $\mathbf{y} \cdot \mathbf{z} = \sum_{i=1}^d y_i z_i$, $\forall \mathbf{y} = \{y_i\}_{i=1}^d$, $\mathbf{z} = \{z_i\}_{i=1}^d \in \mathbb{R}^d$).

2.2. Time discretization of the Stokes problem (2.1)–(2.4)

With $\Delta t(>0)$ a *time discretization* step, we approximate the time dependent Stokes problem (2.1)–(2.4) by the following *backward Euler scheme* (we consider that particular scheme essentially for its simplicity, but more accurate ones are available leading to the same type of elliptic problems at each time step):

$$\frac{\mathbf{u}^{n+1} - \mathbf{u}^n}{\Delta t} - \nu \nabla^2 u^{n+1} + \nabla p^{n+1} = \mathbf{f}^{n+1} \qquad \text{in } \Omega, \tag{2.8}$$

$$\nabla \cdot \mathbf{u}^{n+1} = 0 \qquad \text{in } \Omega, \tag{2.9}$$

$$\mathbf{u}^{n+1} = \mathbf{g}^{n+1} \qquad \text{on } \Gamma, \tag{2.10}$$

$$\mathbf{u}^0 = u_0; \tag{2.11}$$

in (2.8)–(2.10), $\mathbf{u}^q(x) \sim \mathbf{u}(x, q\,\Delta t)$, $p^q(x) \sim p(x, q\,\Delta t)$, $\mathbf{f}^q(x) = \mathbf{f}(x, q\,\Delta t)$, $\mathbf{g}^q(x) = \mathbf{g}(x, q\,\Delta t)$. Clearly, the problems to solve at each time step are all particular cases of

$$\alpha \mathbf{u} - \nu \nabla^2 \mathbf{u} + \nabla p = \mathbf{f} \qquad \text{in } \Omega, \tag{2.12}$$

$$\nabla \cdot \mathbf{u} = 0 \qquad \text{in } \Omega, \tag{2.13}$$

$$\mathbf{u} = \mathbf{g} \qquad \text{on } \Gamma, \text{ with } \int_\Gamma \mathbf{g} \cdot \mathbf{n} \, d\Gamma = 0, \tag{2.14}$$

with $\alpha > 0$; the solution of (2.12)–(2.14) will be discussed in the Sections 2.3 and 2.4.

Remark 2.1. Using *operator splitting* techniques for the *time discretization* of the full (nonlinear) *incompressible Navier–Stokes equations* leads also to the solution at each time step of problems such as (2.12)–(2.14), with α still the reciprocal of a time step (see [4] and the references therein for more details).

2.3. A functional equation satisfied by the pressure solution of problem (2.12)–(2.14)

If the data $\mathbf{f}$ and $\mathbf{g}$ are sufficiently smooth then problem (2.12)–(2.14) has a *unique solution* in $(H^1(\Omega))^d \times (L^2(\Omega)/\mathbb{R})$ (typical conditions would be $\mathbf{f} \in (H^{-1}(\Omega))^d$, $\mathbf{g} \in (H^{1/2}(\Gamma))^d$); for the definition and properties of the above (Sobolev) functional spaces, see [8, 9]. From now on, we shall consider the unique pressure p belonging to H, where

$$H = \left\{ q \mid q \in L^2(\Omega), \int_\Omega q \, dx = 0 \right\} \qquad (\text{with } dx = dx_1 \cdots dx_d). \tag{2.15}$$

The best way to understand the mechanism interrelating the pressure and velocity approximations is—from our point of view—to eliminate $\mathbf{u}$ in (2.12)–(2.14); to do this, we first define $\mathbf{u}_0$ as the unique solution of the Dirichlet system

$$\alpha \mathbf{u}_0 - \nu \nabla^2 \mathbf{u}_0 = \mathbf{f} \qquad \text{in } \Omega, \tag{2.16}$$

$$\mathbf{u}_0 = \mathbf{g} \qquad \text{on } \Gamma; \tag{2.17}$$

the above function $\mathbf{u}_0$ is not related to the one in (2.4).

We observe that the pressure p satisfies the functional equation

$$Ap = -\nabla \cdot \mathbf{u}_0, \tag{2.18}$$

where, in (2.18), the (*pseudo-differential*) operator A is defined by

$$Aq = -\nabla \cdot ((\alpha I - \nu \nabla^2)^{-1} \nabla q), \qquad \forall q \in L^2(\Omega); \tag{2.19}$$

in (2.19) the boundary conditions associated to $\alpha I - \nu \nabla^2$ are the *homogeneous Dirichlet boundary conditions*, i.e.,

$$Aq = \nabla \cdot \mathbf{u}_q, \qquad \forall q \in L^2(\Omega), \tag{2.20}$$

where $\mathbf{u}_q$ is the solution of the Dirichlet system

$$\alpha \mathbf{u}_q - \nu \nabla^2 \mathbf{u}_q = -\nabla q \qquad \text{in } \Omega, \tag{2.21}$$

$$\mathbf{u}_q = 0 \qquad \text{on } \Gamma, \tag{2.22}$$

which has a *unique* solution in $(H_0^1(\Omega))^d$. We have

$$\int_\Omega Aq \, dx = \int_\Omega \nabla \cdot \mathbf{u}_q \, dx = \int_\Gamma \mathbf{u}_q \cdot \mathbf{n} \, d\Gamma = 0,$$

which implies in turn that

$$Aq \in H, \qquad \forall q \in L^2(\Omega); \tag{2.23}$$

we also have, $\forall q, q' \in L^2(\Omega)$,

$$\int_\Omega (Aq)\, q' \, dx = \alpha \int_\Omega \mathbf{u}_q \cdot \mathbf{u}_{q'} \, dx + \nu \int_\Omega \nabla \mathbf{u}_q \cdot \nabla \mathbf{u}_{q'} \, dx, \tag{2.24}$$

which implies, combined to (2.23) that A is a *self-adjoint, strongly elliptic isomorphism* from H onto H (see, e.g., [9] for details); thus problem (2.18) has a unique solution in H since

$$\int_\Omega \nabla \cdot \mathbf{u}_0 \, dx = \int_\Gamma \mathbf{g} \cdot \mathbf{n} \, d\Gamma = 0$$

implies that the right-hand side $-\nabla \cdot \mathbf{u}_0$ of (2.18) belongs to H.

From the properties of A, problem (2.18) (and therefore the Stokes problem (2.12)–(2.14)) can be solved by *conjugate gradient algorithm* as shown in, e.g., [1, 4, 10] (see also the references therein). In the following Section 2.4, we shall discuss the *space discretization* of operator A.

2.4. Space approximation of Operator A

For simplicity, we consider the particular case where $\Omega = (0, 1) \times (0, 1)$; we define the space discretization step h as $h = 1/(I+1)$, where I is a positive integer, and introduce the *grid points* $M_{ij} = \{ih, jh\}$, $0 \leqslant i, j \leqslant I+1$; the points M_{ij} can be used to define either *finite difference* or *finite element* approximations of problems (2.12)–(2.14) and (2.18). For further simplicity, we shall consider finite difference approximations but the following discussion could have been done in a *finite element* framework, using *piecewise linear approximations* associated to the triangulation of Fig. 2.1 and the trapezoidal rule to evaluate integrals like $\alpha \int_\Omega vw \, dx$ in the corresponding variational formulation of elliptic systems like (2.16), (2.17) and (2.21), (2.22).

The pressure p will be approximated by $p_h = \{p_{ij}\}_{0 \leqslant i,j \leqslant I+1}$ and those velocity fields $\mathbf{v}$ vanishing on Γ, by $\mathbf{v}_h = \{v_{ij}\}_{1 \leqslant i,j \leqslant I}$, with $\mathbf{v}_{ij} \in \mathbb{R}^2$. Let us define the discrete pressure and velocity spaces P_h and V_{0h} by

$$P_h = \{q_h \mid q_h = \{q_{ij}\}_{0 \leqslant i,j \leqslant I+1}\}, \tag{2.25}$$

and

$$V_{0h} = \{\mathbf{v}_h \mid \mathbf{v}_h = \{\mathbf{v}_{ij}\}_{1 \leqslant i,j \leqslant I}, \mathbf{v}_{ij} \in \mathbb{R}^2\}. \tag{2.26}$$

To study the *kernel* and the *damping properties* of the discrete analogue of operator A it is convenient to introduce the following *vector bases* of P_h and V_{0h}:

$$\mathscr{B}_{ph} = \{\varphi_{mn} \mid \varphi_{mn} = \{\cos mi\pi h \times \cos nj\pi h\}_{0 \leqslant i,j \leqslant I+1}, \quad 0 \leqslant m, n \leqslant I+1\} \tag{2.27}$$

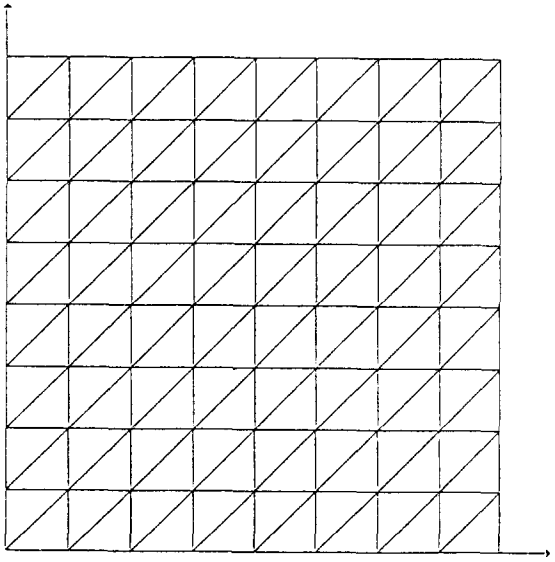

FIG. 2.1. A regular triangulation associated to the grid points M_{ij}.

and

$$\mathscr{B}_{vh} = \{\{\sin mi\pi h \times \sin nj\pi h, 0\}_{1 \leqslant i,j \leqslant I},$$
$$1 \leqslant m, n \leqslant I\} \cup \{\{0, \sin ki\pi h \times \sin lj\pi h\}_{1 \leqslant i,j \leqslant I},$$
$$1 \leqslant k, l \leqslant I\}, \tag{2.28}$$

respectively.

The convenience of the above bases is due to the fact that their elements are the *eigenvectors* of matrices which approximate (via finite difference discretizations) the elliptic operator $-\nabla^2$ for the homogeneous Neumann and Dirichlet boundary conditions, respectively. The finite difference method to be described below is not used in practice (until recently at least) since it is known to be unstable. However, since the corresponding discretization is very close to the one obtained by finite element methods using regular triangulations such the one in Fig. 2.1, and on these triangulations piecewise linear approximations for both pressure and velocity, we shall consider it in detail. Indeed, the crucial part is the way $(\alpha I - \nu\nabla^2)^{-1}\nabla p$ is approximated:

First, if $p_h \in P_h$ we approximate ∇p at M_{ij} by

$$(\delta p_h)_{ij} = \left\{\frac{p_{i+1j} - p_{i-1j}}{2h}, \frac{p_{ij+1} - p_{ij-1}}{2h}\right\},$$
$$1 \leqslant i, j \leqslant I. \tag{2.29}$$

If we denote by $\mathbf{w}_h$ the element of V_{0h} approximating $(\alpha I - \nu\nabla^2)^{-1}\nabla p$, we obtain it via the solution of the linear system

$$\alpha \mathbf{w}_{ij} - \frac{\nu}{h^2}(\mathbf{w}_{i+1j} + \mathbf{w}_{i-1j} + \mathbf{w}_{ij+1} + \mathbf{w}_{ij-1} - 4\mathbf{w}_{ij})$$
$$= (\delta p_h)_{ij}, \qquad 1 \leqslant i, j \leqslant I. \tag{2.30}$$

To study the properties of the mapping

$$p_h \to \mathbf{w}_h : P_h \to V_{0h}, \tag{2.31}$$

we consider the particular case, where $p_h = \varphi_{mn} \in \mathscr{B}_{ph}$; the corresponding value of $(\delta p_h)_{ij}$, denoted by $(\delta\varphi_{mn})_{ij}$ is then given by

$$(\delta\varphi_{mn})_{ij} = -\left\{\frac{\sin m\pi h}{h} \sin mi\pi h \times \cos nj\pi h,\right.$$
$$\left.\frac{\sin n\pi h}{h} \cos mi\pi h \times \sin nj\pi h\right\}. \tag{2.32}$$

Relation (2.32) is the discrete analogue of

$$\nabla\tilde{\varphi}_{mn}(M_{ij}) = -\{m\pi \sin mi\pi h \times \cos nj\pi h,$$
$$n\pi \cos mi\pi h \times \sin nj\pi h\},$$

where the function $\tilde{\varphi}_{mn}$ is defined by $\tilde{\varphi}_{mn}(x_1, x_2) = \cos m\pi x_1 \cos n\pi x_2$.

If $m = n = I + 1$, we clearly have $(\delta\varphi_{mn})_{ij} = 0$, $\forall 1 \leqslant i, j \leqslant I$; indeed, relation (2.32) tells us more since it follows from Fig. 2.2 (where we have visualized, with an appropriate scaling, the function $m\pi \to m\pi$ and its discrete analogue, namely the function $m\pi \to \sin m\pi h/h$), that for $m, n > (I+1)/2$, the vectors φ_{mn} are *strongly damped* by the finite difference approximation of ∇ defined by (2.29). If we consider now the matrix in the left-hand side of (2.30), it is quite easy to check that its *eigenvectors* are either

$$\{\sin mi\pi h \times \sin nj\pi h, 0\}_{1 \leqslant i,j \leqslant I}, \qquad 1 \leqslant m, n \leqslant I, \tag{2.33}$$

or

$$\{0, \sin mi\pi h \times \sin nj\pi h\}_{1 \leqslant i,j \leqslant I}, \qquad 1 \leqslant m, n \leqslant I, \tag{2.34}$$

the corresponding eigenvalues being

$$\alpha + \frac{4\nu}{h^2}\left(\sin^2 m\frac{\pi}{2}h + \sin^2 n\frac{\pi}{2}h\right). \tag{2.35}$$

Since $\mathbf{w}_h$ is obtained by multiplying the right-hand side of (2.30) by the inverse of the above matrix, we observe from (2.35) that the damping of the high wave number modes of p_h associated to the discretization of ∇ is further amplified; actually the traditional finite difference discretizations of the divergence operator have a similar behavior (a related discussion concerning spectral approximations of the Stokes problem can be found in, e.g., [11, 12]).

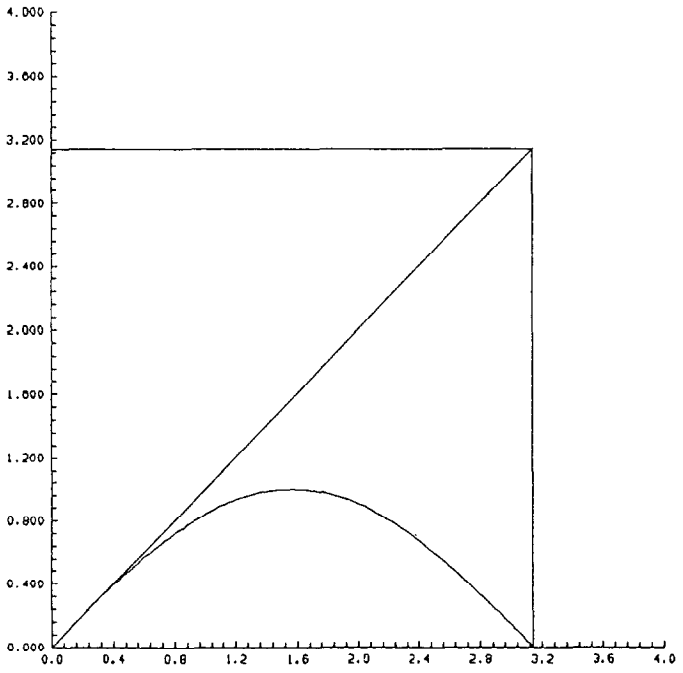

FIGURE 2.2

To summarize the above analysis we can say that the pressure modes such that m and/or $n > (I+1)/2$ are strongly damped by the discrete analogue of the operator A defined by (2.19); this property implies that spurious pressure and velocity oscillations are produced if one relies on the above approach to solve the Stokes problem (2.12)–(2.14), via (2.18). Actually, the finite element approximations of (2.12)–(2.14), which use the same mesh and type of finite elements for pressure and velocity, have the same drawbacks that the finite difference method, which has been described above (we insist on the fact that this method is essentially equivalent to a finite element one, using piecewise linear approximations for pressure and velocity on triangulations such the one in Fig. 2.1). To overcome the above unstability we can either

(a) Use different types of approximations for pressure and velocity

or

(b) Use the same type of approximation for pressure and velocity, combined to a regularization procedure.

Approach (a) is well known and is related to the so-called *inf-sup condition*; finite element approximations which satisfy it are discussed in, e.g., [10, 13–18]; the main idea here is to construct pressure spaces which are "poor" in high frequency modes, compared to the velocity space. Figure 2.2 suggests an obvious remedy which is to use a pressure grid which is *twice coarser* than the velocity grid, and then use approximations of the same type on both grids. This observation makes sense for finite difference, finite element, and wavelet approximations of problem (2.12)–(2.14); the well-known (and converging) finite element method obtained by using a *continuous piecewise linear* approximation of the *pressure* (resp. of the *velocity*) on a triangulation $\mathcal{T}_h$ (resp. $\mathcal{T}_{h/2}$, obtained from $\mathcal{T}_h$ by joining, as shown in Fig. 2.3, the midpoints in any $T \in \mathcal{T}_h$) definitely follows the above rule. This method is discussed in [1, 4, 13–18] (some of the above references show numerical results obtained with it).

Approach (b) which has been recently strongly advocated by several authors (see, e.g., [19]), leads essentially to

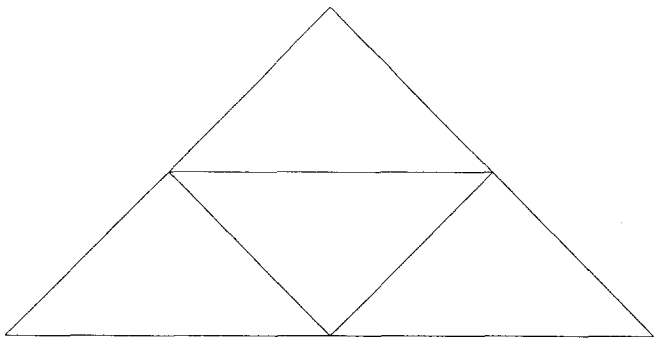

FIGURE 2.3

Tychonoff regularization procedures, an obvious one being to "regularize" Eq. (2.18) by the following problem (written in variational form):

$$p_\varepsilon \in H^1(\Omega),$$

$$\varepsilon \int_\Omega \nabla p_\varepsilon \cdot \nabla q \, dx + \int_\Omega (Ap_\varepsilon)\, q \, dx \tag{2.36}$$

$$= -\int_\Omega \nabla \cdot \mathbf{u}_0 q \, dx, \qquad \forall q \in H^1(\Omega),$$

where, in (2.36), ε is a positive parameter.

Very good results have been obtained with approach (b) (see [19]), we prefer, however, approach (a), for the following reasons:

(i) It is *parameter free*, unlike the second approach which requires the adjustment of the regularization parameter ε.

(ii) In general, the mesh size is adjusted, globally or locally, on the basis of the velocity behavior (boundary and shear layer thicknesses, for example). Therefore, compared to approach (a), approach (b) will be four times more costly (eight times for three-dimensional problems) from the pressure point of view, without further gains in accuracy.

(iii) Multilevels solvers have been recently developed for solving problem (2.12)–(2.14); since methods of type (a) have also a multilevel structure concerning the approximation of pressure and velocity, we think that they are better suited than those of type (b) for multilevel solution methods such as multigrid.

(iv) Tychonoff regularization procedures are systematic methods for stabilizing ill-posed problems; in most cases, the adjustment of the regularization parameter is a delicate problem in itself; therefore if there exist alternatives which are parameter free we definitely think that the latter are preferable, particularly if they are based on an analysis of the mechanism producing the unwanted oscillations. Actually, we have nothing against regularization procedures since we have been using them, in [3, 4], to solve control problems like the one discussed in the following Sections 3 and 4; however, as a result of the present analysis, we shall discuss in Section 3 (in the spirit of the methods of type (a)), new solution methods for the above control problems, which are more efficient than those discussed in [3, 4].

2.5. A Remark on the Stokes Problem with Periodic Boundary Conditions

Suppose that Ω is the square $(0, 1)^2$ and consider (with α still positive) the following variant of the Stokes problem (2.12)–(2.14):

$$\alpha \mathbf{u} - \nu \nabla^2 \mathbf{u} + \nabla p = \mathbf{f} \quad \text{in } \Omega, \tag{2.37}$$

$$\nabla \cdot \mathbf{u} = 0 \quad \text{in } \Omega, \tag{2.38}$$

$$\mathbf{u}(x_1, 0) = \mathbf{u}(x_1, 1), \quad \mathbf{u}(0, x_2) = \mathbf{u}(1, x_2), \quad 0 < x_1, x_2 < 1, \tag{2.39}$$

$$\nabla \mathbf{u}(x_1, 0) = \nabla \mathbf{u}(x_1, 1), \quad \nabla \mathbf{u}(0, x_2) = \nabla \mathbf{u}(1, x_2), \quad 0 < x_1, x_2 < 1; \tag{2.40}$$

the boundary conditions (2.39), (2.40) are of *periodic type.*

It is well known (particularly to the spectral methods specialists) that solving problem (2.37)–(2.40) is fairly easy; however since this fact seems to be much less known to finite element people, we discuss here with some detail the solution of problem (2.37)–(2.40).

We suppose that $\mathbf{f} \in (L^2(\Omega))^2$. Taking the divergence of both sides of (2.37) we obtain from (2.38) that

$$\nabla^2 p = \nabla \cdot \mathbf{f} \quad \text{in } \Omega. \tag{2.41}$$

Assuming that p is periodic in the sense of (2.39), (2.40), it is also a solution of the following variational problem

$$p \in P, \quad \int_\Omega \nabla p \cdot \nabla q \, dx = \int_\Omega \mathbf{f} \cdot \nabla q \, dx, \quad \forall q \in P, \tag{2.42}$$

where P is the subspace of $H^1(\Omega)$, consisting of those functions periodic at Γ in the sense of (2.39). Applying the Lax–Milgram theorem (cf., e.g., [18, Appendix 1]) to problem (2.42), we obtain that problem (2.42) has a unique solution in $P/\mathbb{R}$ (i.e., defined within to an additive constant). Once p is known, we compute $\mathbf{u}$ as the solution of the elliptic system

$$\alpha \mathbf{u} - \nu \nabla^2 \mathbf{u} = \mathbf{f} - \nabla p \quad \text{in } \Omega, \tag{2.43}$$

completed by the boundary conditions (2.39), (2.40). Problem (2.43), (2.39), (2.40) has a unique solution, whose divergence is itself periodic. Denote $\nabla \cdot \mathbf{u}$ by φ and observe that φ satisfies (from (2.41))

$$\alpha \varphi - \nu \nabla^2 \varphi = 0 \quad \text{in } \Omega, \tag{2.44}$$

which, combined to the periodicity conditions satisfied by φ, implies that $\varphi = \nabla \cdot \mathbf{u} = 0$ in Ω. We have thus solved problem (2.37)–(2.40). We observe therefore that solving problem (2.37)–(2.40) amounts to solving a fixed small number of very simple elliptic problems.

Actually this simplicity of the Stokes problem (2.37)–(2.40) is preserved by discretization; we can use different approximation methods to compute pressure and velocity, we can use different meshes, we can combine spectral methods for one of the unknown function to finite element methods for the other, we can also use similar approximations on the same grid, etc. This extreme robustness of the periodic Stokes problem (2.37)–(2.40) with respect to its numerical solution is not shared by the Stokes/Dirichlet problem (2.12)–(2.14). However, efficient numerical methods for solving problem (2.12)–(2.14) have been developed these last years; they combine, for example, finite element approximations for pressure and velocity (piecewise linear pressure, piecewise quadratic velocity, for example) to very efficient preconditioned conjugate gradient algorithms like those introduced in [19] and discussed with further details in, e.g., [10, 15]. Indeed these algorithms are particular cases of a general methodology for some class of linear variational problems to be discussed in Section 3; therefore, for the sake of completeness we shall come back to them in the Appendix and describe there a generalization to situations where in addition to Eqs. (2.12), (2.13), boundary conditions such as

$$\nu \frac{\partial \mathbf{u}}{\partial \mathbf{n}} - \mathbf{n} p = \mathbf{g} \tag{2.45}$$

hold on a part of the boundary Γ.

3. ON THE EXACT BOUNDARY CONTROLLABILITY OF THE WAVE EQUATION

3.1. Introduction: Synopsis

Inverse problems for partial differential equations have always been challenging ones, both from the theoretical and computational points of view. Indeed, they have the justified reputation of being very computer time consuming. Among these inverse problems, control problems for partial differential equations occupy a very particular niche, and indeed, those last years have seen a renewed interest in exact controllability problems for the wave equations and other equations modelling vibration and oscillation phenomena, such as the Maxwell equations, the equations modelling the vibrations of plates, beams, shells, etc. Interest in such problems clearly arises from the current advanced projects on flexible space structures, stealth aerospace vehicles, etc.

In this article, we shall discuss the solution of an exact boundary controllability problem for the wave equation, focussing on approximation issues; the iterative solution of the control problem by conjugate gradient techniques will be addressed also. Concerning more specifically the approximation aspect, it will appear than an efficient way to eliminate unwanted numerical oscillations will be to use two different grids (as for the Stokes problem (2.12)–(2.14), and by a similar spectral analysis). In fact, the methods to be discussed in this section provide an efficient and simpler alter-

native to the Tychonoff regularization procedure discussed in [3, 4]. Numerical results will be presented in Section 4.

A (much) shorter version of this article appeared in [21].

3.2. Formulation of the Exact Boundary Controllability Problem

Let Ω be a bounded domain of $\mathbb{R}^d$ ($d \geqslant 1$), with boundary Γ, and for $T>0$, let $(0, T)$ be a time interval. We shall use the following notation

$$x = \{x_i\}_{i=1}^d, \qquad dx = dx_1 \cdots dx_d,$$

$$\nabla = \left\{\frac{\partial}{\partial x_i}\right\}_{i=1}^d,$$

$$\Delta = \nabla^2 = \sum_{i=1}^d \frac{\partial^2}{\partial x_i^2},$$

$$u_t = \frac{\partial u}{\partial t}, \qquad u_{tt} = \frac{\partial^2 u}{\partial t^2},$$

$$\Box = \frac{\partial^2}{\partial t^2} - \Delta, \qquad Q = \Omega \times (0, T),$$

$$\Sigma = \Gamma \times (0, T).$$

Also, we denote by $u(t)$ the function $x \to u(x, t)$. We consider now a physical system governed by the *wave equation*

$$\Box u = 0 \qquad \text{in } Q \tag{3.1}$$

and satisfying the initial conditions

$$u(x, 0) = u^0(x), \qquad u_t(x, 0) = u^1(x) \qquad \text{in } \Omega. \tag{3.2}$$

The exact boundary controllability problem that we consider is to find g defined over Σ such that taking as boundary condition

$$u = \mathbf{g} \qquad \text{on } \Sigma, \tag{3.3}$$

the solution of (3.1), (3.2), (3.3) will satisfy

$$u(x, T) = 0, \qquad u_t(x, T) = 0 \qquad \text{on } \Omega. \tag{3.4}$$

It follows from [5–7, 22, 23], that the above problem has a solution *if one takes T sufficiently large*; indeed, the above result will hold with $g \in L^2(\Sigma)$, even for nonsmooth initial data u^0, u^1 (for example, $u^0 \in L^2(\Omega)$, $u^1 \in H^{-1}(\Omega)$ $(= (H_0^1(\Omega))')$.

Remark 3.1. The above result is not surprising, since Eq. (3.1) describes wave motions with velocity $c = 1$; from that, we can expect that the minimal value of T for which the exact controllability holds is of the order of $\operatorname{diam}(\Omega)/c = \operatorname{diam}(\Omega)$, with

$$\operatorname{diam}(\Omega) = \sup_{x, y \in \Omega} \operatorname{distance}(x, y).$$

Theory (cf., e.g., [6, 7]) and numerical experiments (cf. [3]) justify this prediction; actually if Ω is a disk of radius R (resp. a square with edges of length L) the lower bound of those T for which exact controllability holds is $2R$ (resp. L).

A systematic way for constructing such control g is provided by the *Hilbert uniqueness method* of J. L. Lions (cf. [5–7]), to be described in Section 3.3.

3.3. Description of the J. L. Lions method: the HUM method and the operator $\wedge$

Following J. L. Lions [5–7], we reduce the above exact controllability problem to the problem of identifying initial values for an associated (adjoint, in fact) wave equation. To do this we shall use a method due to J. L. Lions called HUM (the Hilbert uniqueness method); see [6, 7] for more details. Let us introduce $E = H_0^1(\Omega) \times L^2(\Omega)$, $E' = H^{-1}(\Omega) \times L^2(\Omega)$, and then define $\wedge$ operating over E as follows:

Take $\mathbf{e} = \{e^0, e^1\} \in E$ and solve from 0 to T

$$\Box \varphi = 0 \qquad \text{in } Q, \tag{3.5}_1$$

$$\varphi(0) = e^0, \qquad \varphi_t(0) = e^1 \qquad \text{in } \Omega, \tag{3.5}_2$$

$$\varphi = 0 \qquad \text{on } \Sigma; \tag{3.5}_3$$

solve then from T to 0

$$\Box \psi = 0 \qquad \text{in } Q, \tag{3.6}_1$$

$$\psi(T) = 0, \qquad \psi_t(T) = 0 \qquad \text{in } \Omega, \tag{3.6}_2$$

$$\psi = \frac{\partial \varphi}{\partial n}\bigg|_{\Sigma} \qquad \text{on } \Sigma. \tag{3.6}_3$$

We finally define $\wedge$ by

$$\wedge \mathbf{e} = \{\psi_t(0), -\psi(0)\}. \tag{3.7}$$

It is proved in [6, 7] that $\wedge$ is a *linear* and *continuous* operator from E into E'; moreover, if T is *sufficiently large* ($T > T_{\min} \approx \operatorname{diam}(\Omega)$), then it is proved in the above two references that $\wedge$ is an *isomorphism* from E onto E'.

Application to the Exact Boundary Controllability of the Wave Equation (3.1) *for the Intial Conditions* (3.2)

Suppose that $u^0 \in L^2(\Omega)$, $u^1 \in H^{-1}(\Omega)$.

Step 1. Take $\mathbf{f} = \{u^1, -u^0\}$.

Step 2. Solve

$$\bigwedge \mathbf{e} = \mathbf{f}. \tag{3.8}$$

Step 3. Solve the associated wave equation (3.5).

Step 4. Take $g = (\partial\varphi/\partial n)|_\Sigma$.

Step 5. Solve the associated wave equation (3.6).

We have then

$$\Box\psi = 0 \quad \text{in } Q, \qquad \psi = g \quad \text{on } \Sigma,$$
$$\psi(0) = u^0, \qquad \psi_t(0) = u^1, \qquad \psi_t(T) = 0, \qquad \text{in } \Omega.$$

Taking $u = \psi$, it is quite clear that we have computed a g for which we have the exact boundary controllability property.

Further Comments

1. In the sequel of this paper we shall be mostly concerned with the solution of $\bigwedge \mathbf{e} = \mathbf{f}$.

2. Using the HUM approach we have already mentioned that the original control problem is transformed to an *identification of initial conditions problem.* In fact, it can be shown (see [6, 7]) that problem $\bigwedge \mathbf{e} = \mathbf{f}$ is in *duality* with the minimization problem

$$\min_{v \in \mathcal{U}_{ad}} \int_\Sigma v^2 \, d\Gamma \, dt, \tag{3.9}$$

where

$$\mathcal{U}_{ad} = \{v \mid v \in L^2(\Sigma),\ \Box y = 0 \text{ in } Q,\ y = v \text{ on } \Sigma,$$
$$y(0) = u^0,\ y_t(0) = u^1,\ y(T) = 0,\ y_t(T) = 0\}.$$

Indeed, the control g built via HUM is the *unique* solution of the minimization problem (3.9).

3.4. Further properties of $\bigwedge$

3.4.1. *Symmetry and Positivity*

Integrating by parts in time and using the divergence theorem, we should easily prove that

$$\left\langle \bigwedge \mathbf{e}, \check{\mathbf{e}} \right\rangle = \int_\Omega (\psi_t(x,0)\,\check{\varphi}(x,0) - \psi(x,0)\,\check{\varphi}_t(x,0))\,dx$$
$$= \int_\Sigma \frac{\partial\varphi}{\partial n}\frac{\partial\check{\varphi}}{\partial n}\,d\Gamma\,dt, \qquad \forall \mathbf{e}, \check{\mathbf{e}} \in E, \tag{3.10}$$

where, in (3.10), $\langle \cdot, \cdot \rangle$ denotes the duality pairing between E' and E (i.e., the generalized scalar product between the elements of E' and those of E). It follows from (3.10) that $\bigwedge$ is *self-adjoint*, and *strongly elliptic* if T is *sufficiently large.*

3.4.2. *Asymptotic Behavior*

Suppose that there exist $x_0 \in \Omega$ and $C > 0$ such that

$$\overline{x_0 M} \cdot \mathbf{n} = C, \qquad \forall M \in \Gamma, \tag{3.11}$$

with $\mathbf{n}$ the unit vector of the outward normal at Γ, at M. Domains satisfying (3.11) are easy to characterize geometrically, simple cases being disks and squares. Now let us denote by $\bigwedge_T$ the operator $\bigwedge$ associated to T. It has been shown by J. L. Lions [24] (see also Bensoussan [25]) that

$$\lim_{T \to +\infty} \frac{\bigwedge_T}{T} = \frac{1}{C}\begin{bmatrix} -\Delta & 0 \\ 0 & I \end{bmatrix}. \tag{3.12}$$

Result (3.12) is quite important for the validation of the numerical methods described below, since it easily provides

$$\lim_{T \to +\infty} T\mathbf{e}_T = \{\chi^0, \chi^1\}, \tag{3.13}$$

where, from (3.12),

$$-\Delta\chi^0 = Cu^1 \quad \text{in } \Omega, \qquad \chi^0 = 0 \quad \text{on } \Gamma, \tag{3.14}$$
$$\chi^1 = -Cu^0. \tag{3.15}$$

3.5. Conjugate Gradient Solution of the Problem $\bigwedge \mathbf{e} = \mathbf{f}$

3.5.1. *Generalities on the Conjugate Gradient Solution of Linear Variational Problems in Hilbert Spaces*

Problem $\bigwedge \mathbf{e} = \mathbf{f}$ can also be written

$$\mathbf{e} \in E, \qquad \left\langle \bigwedge \mathbf{e}, \check{\mathbf{e}} \right\rangle = \langle \mathbf{f}, \check{\mathbf{e}} \rangle, \qquad \forall \check{\mathbf{e}} \in E, \tag{3.16}$$

where, in (3.16), $\langle \cdot, \cdot \rangle$ denotes the duality pairing mentioned above. Suppose now that T is sufficiently large, then the bilinear form $\langle \bigwedge \cdot, \cdot \rangle$ is, from Section 3.4.1, continuous, symmetric, and E-elliptic; i.e., there exists $\gamma > 0$ such that

$$\left\langle \bigwedge \check{\mathbf{e}}, \check{\mathbf{e}} \right\rangle \geq \gamma \, \|\check{\mathbf{e}}\|_E^2, \qquad \forall \check{\mathbf{e}} \in E, \tag{3.17}$$

with, in (3.17),

$$\|\check{\mathbf{e}}\|_E = \left(\int_\Omega (|\nabla \check{e}^0|^2 + |\check{e}^1|^2)\,dx \right)^{1/2}$$
$$\forall \check{\mathbf{e}} = \{\check{e}^0, \check{e}^1\} \in E.$$

Problem (3.16) is therefore a particular case of the family of linear variational problems,

$$u \in V, \qquad a(u, v) = L(v), \qquad \forall v \in V, \tag{P}$$

where in (P):

(i) V is a real *Hilbert space* for the *scalar product* $(\cdot, \cdot)$ and the corresponding norm $\|\cdot\|$.

(ii) $a: V \times V \to \mathbb{R}$ is *bilinear, continuous, symmetric* (i.e., $a(v, w) = a(w, v)$, $\forall v, w \in V$) and *V-elliptic* (i.e., there exists $\alpha > 0$ such that $a(v, v) \geq \alpha \|v\|^2$, $\forall v \in V$).

(iii) $L: V \to \mathbb{R}$ is *linear* and *continuous*.

With the above hypotheses problem (P) has a *unique* solution (cf., e.g., [18, Appendix 1]), which can be computed by the following *conjugate gradient* algorithm:

Step 0. *Initialization.*

$$u^0 \in V \text{ is given;} \tag{3.18}$$

solve then

$$g^0 \in V, \qquad (g^0, v) = a(u^0, v) - L(v), \qquad \forall v \in V. \tag{3.19}$$

If $g^0 = 0$, or is "small," take $u = u^0$; if not, set

$$w^0 = g^0. \tag{3.20}$$

Then for $n \geq 0$, assuming that u^n, g^n, w^n are known, compute u^{n+1}, g^{n+1}, w^{n+1} as follows

Step 1. *Descent.* Compute

$$\rho_n = \frac{\|g^n\|^2}{a(w^n, w^n)}, \tag{3.21}$$

and then

$$u^{n+1} = u^n - \rho_n w^n. \tag{3.22}$$

Step 2. *Test of the convergence and construction of the new descent direction.* Solve

$$g^{n+1} \in V,$$
$$(g^{n+1}, v) = (g^n, v) - \rho_n a(w^n, v), \qquad \forall v \in V; \tag{3.23}$$

if $g^{n+1} = 0$, or is "small," take $u = u^{n+1}$; if not, compute

$$\gamma_n = \frac{\|g^{n+1}\|^2}{\|g^n\|^2}, \tag{3.24}$$

and define the new descent direction by

$$w^{n+1} = g^{n+1} + \gamma_n w^n. \tag{3.25}$$

Do $n = n + 1$ and go to (3.21).

If the above assumptions on V, $a(\cdot, \cdot)$, $L(\cdot)$ hold, one can prove that, $\forall u^0 \in V$, one has

$$\lim_{n \to +\infty} \|u^n - u\| = 0, \tag{3.26}$$

where u is the solution of problem (P). In fact, it follows from [26] that we also have

$$\|u^n - u\| \leq C \|u^0 - u\| \left(\frac{\sqrt{\nu_a} - 1}{\sqrt{\nu_a} + 1} \right)^n, \tag{3.27}$$

where the *condition number* ν_a of $a(\cdot, \cdot)$ is defined by

$$\nu_a = \sup_{v \in V - \{0\}} \frac{a(v, v)}{\|v\|^2} : \inf_{v \in V - \{0\}} \frac{a(v, v)}{\|v\|^2}.$$

Remark 3.2. For finite dimensional problems (P), algorithm (3.18)–(3.25) is nothing but a preconditioned conjugate gradient algorithm for solving a linear system.

Remark 3.3. The choice of a proper scalar product over V is a critical factor for the convergence properties of the conjugate gradient algorithm (3.18)–(3.25); indeed we expect from $(\cdot, \cdot)$ to be sufficiently close to $a(\cdot, \cdot)$ so that the above condition number ν_a will be of the order of 1; on the other hand, to make algorithm (3.18)–(3.25) of practical interest the linear problems associated to $(\cdot, \cdot)$ (such as (3.19) and (3.23)) have to be much cheaper to solve than the ones associated to $a(\cdot, \cdot)$. The art of preconditioning is precisely to find the right compromise between these seemingly contradictory properties of the scalar product $(\cdot, \cdot)$. It seems that in the particular case of the control problem presently discussed (and also of the Stokes problem (2.12)–(2.14) (see the Appendix)) the right scalar product has been identified.

Remark 3.4. Back to the practical implementation of algorithm (3.18)–(3.25), by g^0 (resp. g^{n+1}) "small" we essentially mean that g^0 (resp. g^{n+1}) satisfies

$$\|g^0\| / \|u^0\| \leq \varepsilon \text{ (resp. } \|g^{n+1}\| / \|g^0\| \leq \varepsilon), \tag{3.28}$$

where ε is a small positive number depending upon the floating point arithmetic used by the computer; we have been quite successful, taking $\varepsilon = 10^{-7}$ in (3.28) when running on the CRAY X-MP.

3.5.2. *Application of the Conjugate Gradient Algorithm* (3.18)–(3.25) *to the Boundary Control of the Wave Equation, via the Solution of Problem* $\wedge \mathbf{e} = \mathbf{f}$

Applying the general conjugate gradient algorithm (3.18)–(3.25) to the solution of $\bigwedge \mathbf{e} = \mathbf{f}$, via (3.16), is possible if T is sufficiently large; indeed, it suffices to take

$$V = E,$$

$$a(\cdot,\cdot) = \left\langle \bigwedge \cdot, \cdot \right\rangle, \qquad L: \check{\mathbf{e}} \to \langle \{u^1, -u^0\}, \check{\mathbf{e}} \rangle.$$

On E, we shall use as *scalar product*

$$\{\mathbf{v}, \mathbf{w}\} \to \int_\Omega (\nabla v^0 \cdot \nabla w^0 + v^1 w^1)\, dx, \qquad \forall \mathbf{v}, \mathbf{w} \in E. \tag{3.29}$$

We obtain then the following conjugate gradient algorithm:

Step 0. *Initialization.*

$$e_0^0 \in H_0^1(\Omega) \text{ and } e_0^1 \in L^2(\Omega) \text{ are given;} \tag{3.30}$$

solve then

$$\Box \varphi_0 = 0 \quad \text{in } Q, \qquad \varphi_0 = 0 \quad \text{on } \Sigma,$$
$$\varphi_0(0) = e_0^0, \qquad \frac{\partial \varphi_0}{\partial t}(0) = e_0^1, \tag{3.31}$$

and

$$\Box \psi_0 = 0 \quad \text{in } Q,$$
$$\psi_0 = \frac{\partial \varphi_0}{\partial n}\bigg|_\Sigma \quad \text{on } \Sigma, \tag{3.32}$$
$$\psi_0(T) = 0, \qquad \frac{\partial \psi_0}{\partial t}(T) = 0.$$

Compute $\mathbf{g}_0 = \{g_0^0, g_0^1\} \in E$ by

$$-\nabla^2 g_0^0 = \frac{\partial \psi_0}{\partial t}(0) - u^1 \quad \text{in } \Omega, \tag{3.33}$$
$$g_0^0 = 0 \quad \text{on } \Gamma,$$
$$g_0^1 = u^0 - \psi_0(0), \tag{3.34}$$

respectively. Set then

$$\mathbf{w}_0 = \mathbf{g}_0. \tag{3.35}$$

Now, for $n \geqslant 0$, assuming that $\mathbf{e}_n$, $\mathbf{g}_n$, $\mathbf{w}_n$, φ_n, ψ_n are known, compute $\mathbf{e}_{n+1}$, $\mathbf{g}_{n+1}$, $\mathbf{w}_{n+1}$, φ_{n+1}, ψ_{n+1} as follows:

Step 1. *Descent.* Solve

$$\Box \bar{\varphi}_n = 0 \quad \text{in } Q, \qquad \bar{\varphi}_n = 0 \quad \text{on } \Sigma,$$
$$\bar{\varphi}_n(0) = w_n^0, \qquad \frac{\partial \bar{\varphi}_n}{\partial t}(0) = w_n^1, \tag{3.36}$$

$$\Box \bar{\psi}_n = 0 \quad \text{in } Q,$$
$$\bar{\psi}_n = \frac{\partial \bar{\varphi}_n}{\partial n}\bigg|_\Sigma \quad \text{on } \Sigma, \tag{3.37}$$
$$\bar{\psi}_n(T) = 0, \qquad \frac{\partial \bar{\psi}_n}{\partial n}(T) = 0,$$

$$-\nabla^2 \bar{g}_n^0 = \frac{\partial \bar{\psi}_n}{\partial t}(0) \quad \text{in } \Omega,$$
$$\bar{g}_n^0 = 0 \quad \text{on } \Gamma, \tag{3.38}$$

and set

$$\bar{g}_n^1 = -\bar{\psi}_n(0). \tag{3.39}$$

Compute now

$$\rho_n = \frac{\int_\Omega (|\nabla g_n^0|^2 + |g_n^1|^2)\, dx}{\int_\Omega (\nabla \bar{g}_n^0 \cdot \nabla w_n^0 + \bar{g}_n^1 w_n^1)\, dx}, \tag{3.40}$$

$$\mathbf{e}_{n+1} = \mathbf{e}_n - \rho_n \mathbf{w}_n, \tag{3.41}$$

$$\varphi_{n+1} = \varphi_n - \rho_n \bar{\varphi}_n, \tag{3.42}$$

$$\psi_{n+1} = \psi_n - \rho_n \bar{\psi}_n, \tag{3.43}$$

$$\mathbf{g}_{n+1} = \mathbf{g}_n - \rho_n \bar{\mathbf{g}}_n. \tag{3.44}$$

Step 2. *Test of the convergence and construction of the new descent direction.* If $\mathbf{g}_{n+1} = \mathbf{0}$, or is small, take $\mathbf{e} = \mathbf{e}_{n+1}$, $\varphi = \varphi_{n+1}$, $\psi = \psi_{n+1}$; if not, compute

$$\gamma_n = \frac{\int_\Omega (|\nabla g_{n+1}^0|^2 + |g_{n+1}^1|^2)\, dx}{\int_\Omega (|\nabla g_n^0|^2 + |g_n^1|^2)\, dx}, \tag{3.45}$$

and set

$$\mathbf{w}_{n+1} = \mathbf{g}_{n+1} + \gamma_n \mathbf{w}_n. \tag{3.46}$$

Do $n = n + 1$ and go to (3.40).

Remark 3.5. It appears at first glance that algorithm (3.30)–(3.46) is quite memory demanding since it seems to require the storage of $(\partial \bar{\varphi}_n / \partial n)|_\Sigma$ (in practice the storage of $\partial \bar{\varphi}_n / \partial n$ over a discrete—but still large—subset of Σ). In fact, we can avoid that storage problem by observing that since

the wave equation in (3.36) is *reversible* we can integrate *simultaneously, from T to* 0, the wave equation (3.37) and

$$\begin{aligned} \Box\bar{\varphi}_n &= 0 \qquad \text{in } Q, \\ \bar{\varphi}_n &= 0 \qquad \text{on } \Sigma, \\ \bar{\varphi}_n(T) \text{ and } &\frac{\partial\bar{\varphi}_n}{\partial t}(T) \text{ known from the integration} \\ &\text{of (3.36) from 0 to } T. \end{aligned} \tag{3.47}$$

In the particular case where an *explicit scheme* is used for solving the wave equations (3.36), (3.37), and (3.47), the extra cost associated to the solution of (3.47) is *negligible* compared to the saving due to not storing $(\partial\bar{\varphi}_n/\partial n)|_\Sigma$. In fact, the above conclusion still holds if one uses a convenient *implicit* scheme.

3.6. Discretization of the Boundary Control Problem

3.6.1. *Generalities*

A finite element/finite difference approximation of the above boundary control problem is discussed in [3]. At the present moment, we shall concentrate on the case, where $\Omega = (0, 1)^2$ and where *finite difference* methods are used both for the space and time discretizations. Indeed, these approximations can also be obtained via space discretizations associated to finite element grids like the one shown on Fig. 2.1 (we should use, as shown in [3], piecewise linear approximations and numerical integration by the trapezoidal rule).

Let I and N be positive integers; we define h (*space discretization step*) and Δt (*time discretization step*) by

$$h = 1/(I+1), \qquad \Delta t = T/N, \tag{3.48}$$

respectively, and then denote by M_{ij} the point $\{ih, jh\}$.

3.6.2. *Approximation of the Wave Equation* (3.5)

Let us consider the wave equation (3.5), i.e.,

$$\begin{aligned} \Box\varphi &= 0 \qquad \text{in } Q, \qquad \varphi = 0 \qquad \text{on } \Sigma; \\ \varphi(x, 0) &= e^0(x), \\ \varphi_t(x, 0) &= e^1(x) \qquad \text{on } \Omega. \end{aligned} \tag{3.49}$$

With φ_{ij}^n an approximation of $\varphi(M_{ij}, n\,\Delta t)$, we approximate (3.49) by the following explicit finite difference scheme:

$$\frac{\varphi_{ij}^{n+1} + \varphi_{ij}^{n-1} - 2\varphi_{ij}^n}{|\Delta t|^2} - \frac{\varphi_{i+1\,j}^n + \varphi_{i-1\,j}^n + \varphi_{ij+1}^n + \varphi_{ij-1}^n - 4\varphi_{ij}^n}{h^2} = 0, \tag{3.50}_1$$

$$1 \leqslant i, j \leqslant I, \; 0 \leqslant n \leqslant N,$$

$$\varphi_{kl}^n = 0 \qquad \text{if} \quad M_{kl} \in \Gamma, \tag{3.50}_2$$

$$\begin{aligned} \varphi_{ij}^0 &= e^0(M_{ij}), \\ \varphi_{ij}^1 - \varphi_{ij}^{-1} &= 2\,\Delta t\, e^1(M_{ij}), \qquad 1 \leqslant i, j \leqslant I. \end{aligned} \tag{3.50}_3$$

The above scheme satisfies the *stability condition*

$$\Delta t \leqslant h/\sqrt{2}. \tag{3.51}$$

3.6.3. *Approximation of* $(\partial\varphi/\partial n)|_\Sigma$

Suppose that we want to approximate $\partial\varphi/\partial n$ at $M \in \Gamma$, as shown in Fig. 3.1. Suppose that φ is known at E; we shall then approximate $\partial\varphi/\partial n$ at M by

$$\frac{\partial\varphi}{\partial n}(M) \approx \frac{\varphi(E) - \varphi(W)}{2h}. \tag{3.52}$$

In fact, $\varphi(E)$ is not known since $E \notin \bar{\Omega}$. However—formally at least—$\varphi = 0$ on Σ implies $\varphi_{tt} = 0$ on Σ, which combined with $\varphi_{tt} - \Delta\varphi = 0$ implies $\Delta\varphi = 0$ on Σ; discretizing this last relation at M yields

$$\frac{\varphi(W) + \varphi(E) + \varphi(S) + \varphi(N) - 4\varphi(M)}{h^2} = 0. \tag{3.53}$$

Since N, M, S belong to Γ, (3.53) reduces to

$$\varphi(W) = -\varphi(E), \tag{3.54}$$

which combined to (3.52) implies that

$$\frac{\partial\varphi}{\partial n}(M) \approx -\frac{\varphi(W)}{h} = \frac{0 - \varphi(W)}{h} = \frac{\varphi(M) - \varphi(W)}{h}. \tag{3.55}$$

In that particular case, the *symmetric* approximation (3.52) (which is *second-order accurate*) coincides with the *one-sided* one in (3.55) (which is only *first-order accurate*, in general). In the sequel, we shall use, therefore, (3.55) to approximate $\partial\varphi/\partial n$ at M and we shall denote by $\delta_{kl}\varphi$ the corresponding approximation of $\partial\varphi/\partial n$ at $M_{kl} \in \Gamma$.

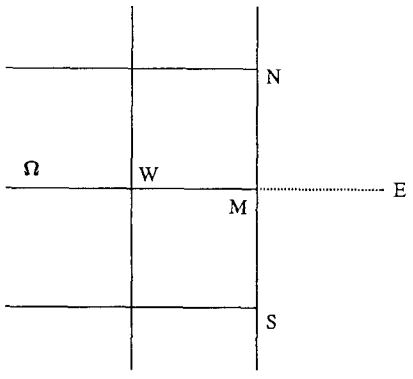

FIGURE 3.1

3.6.4. *Approximation of the Wave Equation* (3.6)

Similarly to (3.5), the wave equation (3.6) will be approximated by

$$\frac{\psi_{ij}^{n-1}+\psi_{ij}^{n+1}-2\psi_{ij}^{n}}{|\Delta t|^2} - \frac{\psi_{i+1j}^{n}+\psi_{i-1j}^{n}+\psi_{ij+1}^{n}+\psi_{ij-1}^{n}-4\psi_{ij}^{n}}{h^2}=0,$$

$$1\leqslant i,j\leqslant I,\ n=N,N-1,\ldots,0, \qquad (3.56)_1$$

$$\psi_{kl}^{n}=\delta_{kl}\varphi^{n} \quad \text{if} \quad M_{kl}\in\Gamma, \qquad (3.56)_2$$

$$\psi_{ij}^{N}=0, \quad \frac{\psi_{ij}^{N+1}-\psi_{ij}^{N-1}}{2\Delta t}=0, \quad 1\leqslant i,j\leqslant I. \qquad (3.56)_3$$

3.6.5. *Approximation of* $\bigwedge$

Starting from

$$\mathbf{e}_h=\{\{e_{ij}^0,\ e_{ij}^1\}\}_{1\leqslant i,j\leqslant I},$$

and via the solution of the discrete wave equations (3.50) and (3.56) we approximate $\bigwedge \mathbf{e}$ by

$$\overset{\Delta t}{\underset{h}{\bigwedge}}\mathbf{e}_h=\left\{\left\{\frac{\psi_{ij}^{1}-\psi_{ij}^{-1}}{2\Delta t},\ -\psi_{ij}^{0}\right\}\right\}_{1\leqslant i,j\leqslant I}. \qquad (3.57)$$

It is proved in [3, pp. 17–19] that we have (with obvious notation)

$$\left\langle \overset{\Delta t}{\underset{h}{\bigwedge}}\mathbf{e}_h,\ \check{\mathbf{e}}_h\right\rangle = h^2\sum_{1\leqslant i,j\leqslant I}\left[\left(\frac{\psi_{ij}^{1}-\psi_{ij}^{-1}}{2\Delta t}\right)\check{e}_{ij}^{0}-\psi_{ij}^{0}\check{e}_{ij}^{1}\right] = h\,\Delta t\sum_{n=0}^{N}\alpha_n\sum_{M_{kl}\in\Gamma^*}\delta_{kl}\varphi^{n}\delta_{kl}\check{\varphi}^{n}, \qquad (3.58)$$

where, in (3.58), $\alpha_0=\alpha_N=\frac{1}{2}$, $\alpha_n=1$, $\forall n=1,\ldots,N-1$, and where $\Gamma^*=\Gamma$ minus the four corners $\{0,0\}$, $\{0,1\}$, $\{1,0\}$, $\{1,1\}$. It follows from (3.58) that $\bigwedge_h^{\Delta t}$ is *symmetric* and *positive-semidefinite*. Actually, it is proved in [3, Section 6.2] that $\bigwedge_h^{\Delta t}$ is *positive definite* if $T>T_{\min}\approx\Delta t/h$. This property implies that if $T(>0)$ is given, it suffices to take $\Delta t/h$ sufficiently small to have the exact boundary controllability for the discrete wave equation. This property is in contradiction with the continuous case where the exact controllability property is lost if T is too small ($T<1$ here). The reasons for this discrepancy will be discussed in the sequel.

3.6.6. *Approximation of* $\bigwedge \mathbf{e}=\mathbf{f}$

With $\mathbf{f}_h$ a convenient approximation of $\mathbf{f}=\{u^1,\ -u^0\}$, we approximate problem $\bigwedge \mathbf{e}=\mathbf{f}$ by

$$\overset{\Delta t}{\underset{h}{\bigwedge}}\mathbf{e}_h=\mathbf{f}_h. \qquad (3.59)$$

In [3, Section 6.3], one may find a discrete variant of the conjugate gradient algorithm (3.30)–(3.46) which can be used to solve the approximate problem (3.59).

3.7. Numerical Solution of a Test Problem; Ill-Posedness of the Discrete Problem (3.59)

Following [3, Section 7; 4, Section 3.7] we still consider the case $\Omega=(0,1)^2$, with $T=15/4\sqrt{2}$ (strictly larger than $\text{diam}(\Omega)=\sqrt{2}$) and e^0, e^1 defined by

$$e^0(x_1,x_2)=\sin\pi x_1\sin\pi x_2, \qquad e^1=\pi\sqrt{2}\,e^0. \qquad (3.60)$$

It is shown in [3, Section 7] that using *separation of variable methods* we can compute a *Fourier Series* expansion of $\mathbf{f}=\bigwedge \mathbf{e}$. The functions $u^0(=-f^1)$ and $u^1(=f^0)$ (both computed by *fast Fourier transform*) have been visualized on Figs. 3.2 and 3.3, respectively. From these figures, u^0 is a *Lipschitz continuous function* which is not C^1; similarly, u^1 is *bounded* but *discontinuous*. On Fig. 3.4, we have shown the graph of the function

$$t\to\left\|\frac{\partial\varphi}{\partial n}(t)\right\|_{L^2(\Gamma)},$$

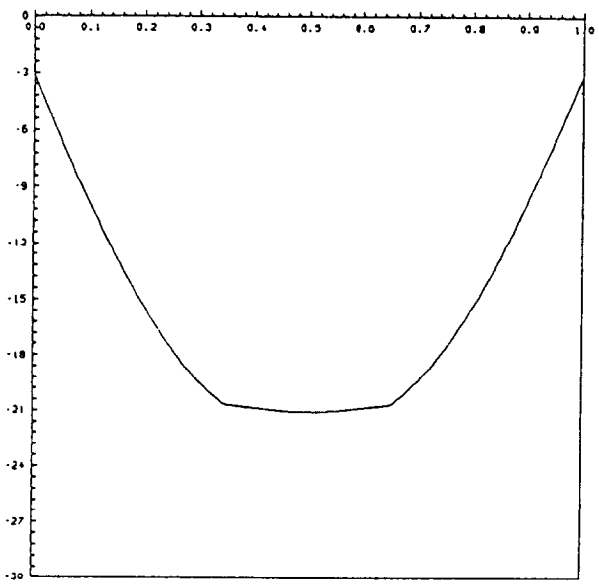

FIG. 3.2. $u^0(x_1, 0.5)$.

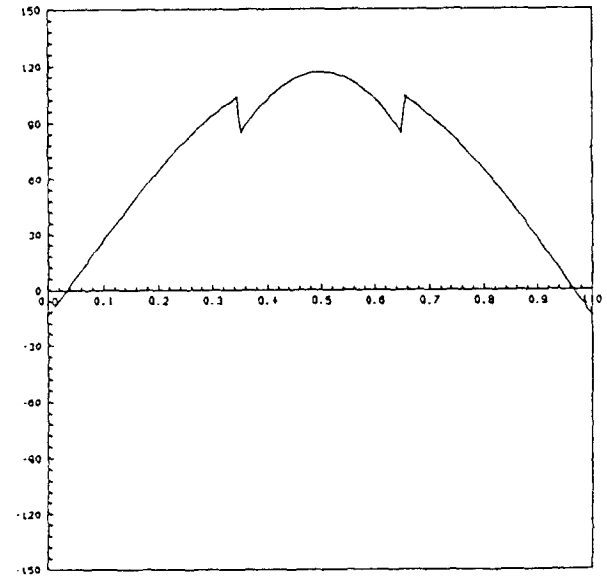

FIG. 3.3. $u^1(x_1, 0.5)$.

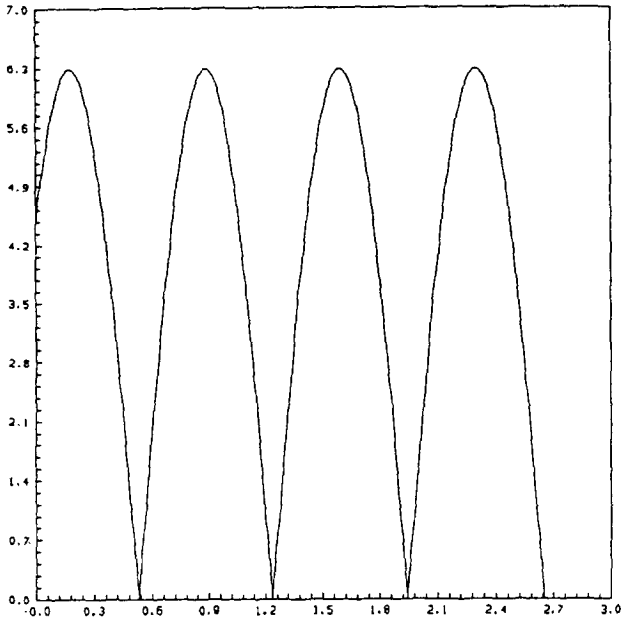

FIG. 3.4. $\|(\partial\varphi/\partial n)(t)\|_{L^2(\Gamma)}$.

where φ, given by

$$\varphi(x, t) = \sqrt{2} \cos \pi \sqrt{2}\left(t - \frac{1}{4\sqrt{2}}\right) \times \sin \pi x_1 \sin \pi x_2, \tag{3.61}$$

is the solution of the wave equation (3.5) when e^0 and e^1 are given by (3.60); we recall that $(\partial\varphi/\partial n)|_\Sigma$ is precisely the Dirichlet control given by HUM (cf. Section 3.3) if the initial conditions u^0 and u^1 satisfy $\{u^1, -u^0\} = \wedge \mathbf{e}$.

The numerical methods described in Sections 3.5 and 3.6 have been applied to the solution of the above test problem taking $\Delta t = h/\sqrt{2}$. Interesting enough, the numerical results deteriorate as h and Δt converge to zero; moreover, taking Δt twice smaller, i.e., $\Delta t = h/2\sqrt{2}$, does not improve the situation. Also, the number of conjugate gradient iterations necessary to achieve convergence increases as h and Δt decrease. Results of our numerical experiments have been summarized in Table I.

In Table I, e_c^0, e_c^1, and g_c are the *computed values* of e^0, e^1, and g, respectively, where $g = (\partial\varphi/\partial n)|_\Sigma$, φ being *the* solution of the wave problem (3.5) associated to the solution $\mathbf{e}$ of $\wedge \mathbf{e} = \mathbf{f}$ (i.e., g is the optimal Dirichlet boundary control).

The most striking fact coming from Table I is the deterioration of the numerical results as h and Δt tend to zero; indeed, for $h = \frac{1}{128}$ the convergence was not achieved after 1000 iterations. This deterioration is obvious from Fig. 3.5 to 3.13, which show for $h = \frac{1}{16}, \frac{1}{32}, \frac{1}{64}$ comparisons between the exact solutions and the computed ones: we have plotted on these figures the values of e^0, e_c^0, e^1, e_c^1 for $x_2 = 0.5$, and also the variation over $[0, T]$ of $\|g(t)\|_{L^2(\Gamma)}$ and $\|g_c(n\,\Delta t)\|_{L^2(\Gamma)}$ (for $n = 0, \ldots, N$). We observe that for $h = \frac{1}{64}$ the variations of e_c^0 and e_c^1 are so large that we have been obliged to use a very large scale to be able to picture them.

If for the same values of h one takes a smaller Δt than $h/\sqrt{2}$ the results remain practically the same. In Section 3.8, we shall try to analyze the reasons of this deterioration of

TABLE I

h	1/8	1/16	1/32	1/64	1/128
Number of conjugate gradient iterations	20	38	84	363.	No convergence
$\|e^0 - e_c^0\|_{L^2(\Omega)}$	0.42×10^{-1}	0.18×10^{-1}	0.41×10^{-1}	3.89	No convergence
$\|e^0 - e_c^0\|_{H_0^1(\Omega)}$	0.65	0.54	2.54	498.1	No convergence
$\|e^1 - e_c^1\|_{L^2(\Omega)}$	0.20	0.64×10^{-1}	1.18	170.6	No convergence
$\|g - g_c\|_{L^2(\Sigma)}$	0.51	0.24	0.24	1.31	No convergence
$\|g_c\|_{L^2(\Sigma)}$	7.320	7.395	7.456	7.520	No convergence

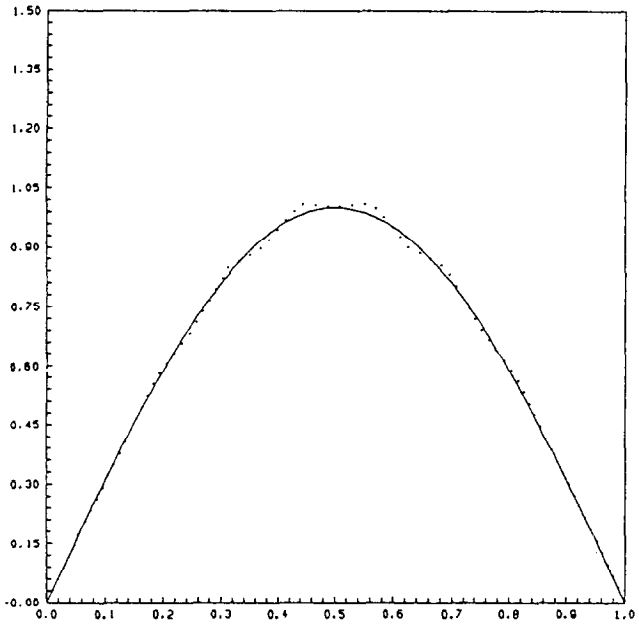

FIG. 3.5. Variations of $e^0(x_1, 0.5)$(—) and $e_c^0(x_1, 0.5)(\cdots)$ $(h = \frac{1}{16})$.

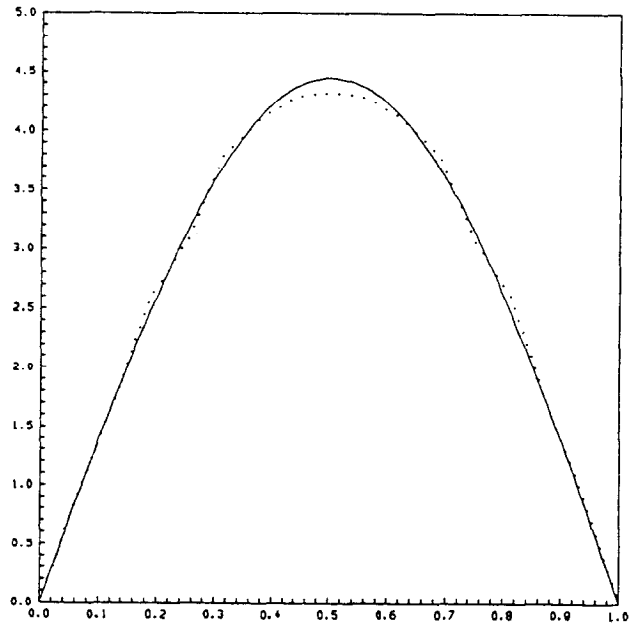

FIG. 3.6. Variations of $e^1(x_1, 0.5)$(—) and $e_c^1(x_1, 0.5)(\cdots)$ $(h = \frac{1}{16})$.

the numerical results as $h \to 0$ and also to give cures for this problem.

To conclude this section we observe that the computed results are quite good for $h = \frac{1}{16}$ and also that the error $\|g - g_c\|_{L^2(\Sigma)}$ deteriorates much more slowly as $h \to 0$ than the errors $e^0 - e_c^0$, $e^1 - e_c^1$; in fact, the approximate values $\|g_c\|_{L^2(\Sigma)}$ of $\|g\|_{L^2(\Sigma)}$ are quite good, even for $h = \frac{1}{64}$ if one realizes that the exact value of $\|g\|_{L^2(\Sigma)}$ is 7.38668...; these relatively good results concerning the behavior of g_c are clear from Figs. 3.7, 3.10, 3.13.

3.8. Analysis and Cure of the Ill-Posedness of the Approximate Problem (3.59)

It follows from the numerical results discussed in Section 3.7, that when h decreases to zero, the *ill-posedness* of the discrete problem is getting worse. From the oscillatory results shown in Figs. 3.5 to 3.13 it is quite clear that the trouble lies with the *high frequency components* of the discrete solution or, to be more precise, with the way the discrete operator $\bigwedge_h^{\Delta t}$ acts on the *short wave length* component of $\mathbf{e}_h$. Before analyzing the mechanism producing those unwanted oscillations let us introduce a vector basis of $\mathbb{R}^{I \times I}$, well suited to the following discussion. This basis $\mathscr{B}_h$ is defined by

$$\mathscr{B}_h = \{w_{pq}\}_{1 \leq p,q \leq I}, \tag{3.62}$$

where

$$w_{pq} = \{\sin p\pi ih \times \sin q\pi jh\}_{1 \leq i,j \leq I}; \tag{3.63}$$

we recall that $h = 1/(I+1)$.

From the oscillatory results described in Section 3.7 it is reasonable to assume that the discrete operator $\bigwedge_h^{\Delta t}$ damps too strongly those components of $\mathbf{e}_h$ with *large wave numbers* p and q; in other words, we can expect that if p and/or q are large, then $\bigwedge_h^{\Delta t}\{w_{pq}, 0\}$ or $\bigwedge_h^{\Delta t}\{0, w_{pq}\}$ will be quite small implying in turn (this is typical of ill-posed problems) that small perturbations of the right-hand side of the discrete problem (3.59) can produce very large variations of the corresponding solution.

Operator $\bigwedge_h^{\Delta t}$ is a fairly complicated one (see Section 3.6

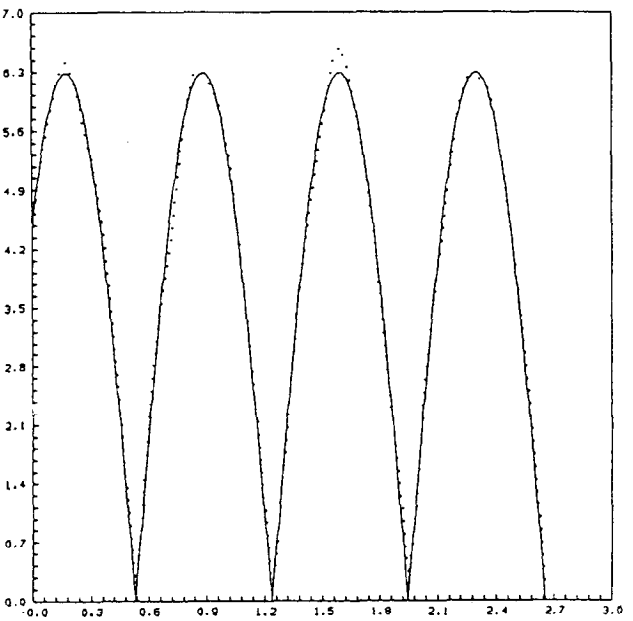

FIG. 3.7. Variations of $\|g(t)\|_{L^2(\Gamma)}$(—) and $\|g_c(t)\|_{L^2(\Gamma)}(\cdots)$ $(h = \frac{1}{16})$.

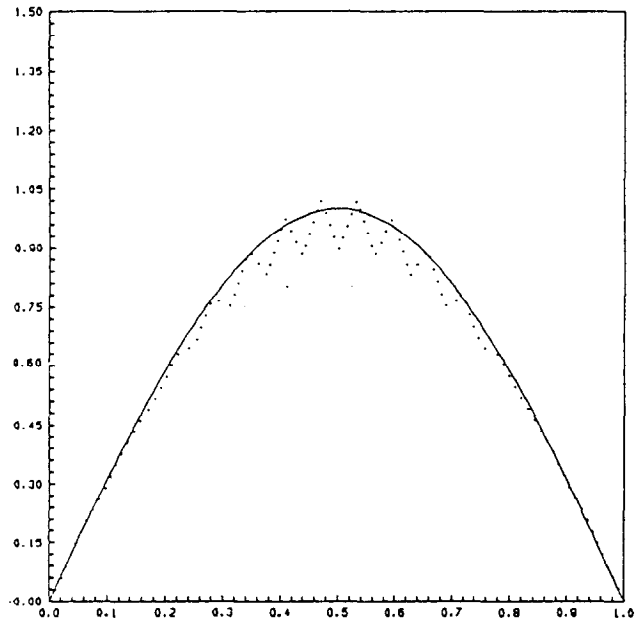

FIG. 3.8. Variations of $e^0(x_1, 0.5)$(—) and $e_c^0(x_1, 0.5)(\cdots)$ $(h = \frac{1}{32})$.

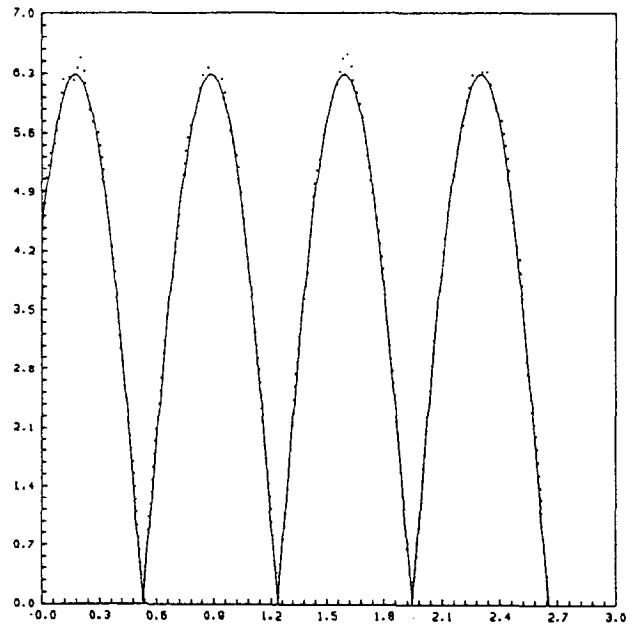

FIG. 3.10. Variations of $\|g(t)\|_{L^2(\Gamma)}$(—) and $\|g_c(t)\|_{L^2(\Gamma)}(\cdots)$ $(h = \frac{1}{32})$.

for its precise definition) and we can wonder which stage in it is particularly acting as a *low pass filter* (i.e., selectively damping the large wave number components of the discrete solutions). Starting from the observation that the ill-posedness persists, if for a fixed h we decrease Δt, it is then natural (and much simpler) to consider the *semi-discrete* case, where only the space derivatives have been discretized.

In such a case, problem (3.5) is discretized as follows (with $\dot{\varphi} = \partial\varphi/\partial t$, $\ddot{\varphi} = \partial^2\varphi/\partial t^2$) if $\Omega = (0, 1)^2$ as in Section 3.6:

$$\ddot{\varphi} - \frac{\varphi_{i+1j} + \varphi_{i-1j} + \varphi_{ij+1} + \varphi_{ij-1} - 4\varphi_{ij}}{h^2} = 0,$$

$$1 \leqslant i, j \leqslant I, \tag{3.64}_1$$

$$\varphi_{kl} = 0 \quad \text{if} \quad \{kh, lh\} \in \Gamma, \tag{3.64}_2$$

$$\varphi_{ij}(0) = e_h^0(ih, jh),$$
$$\dot{\varphi}_{ij}(0) = e_h^1(ih, jh), \qquad \forall i, j,\ 1 \leqslant i, j \leqslant I. \tag{3.64}_3$$

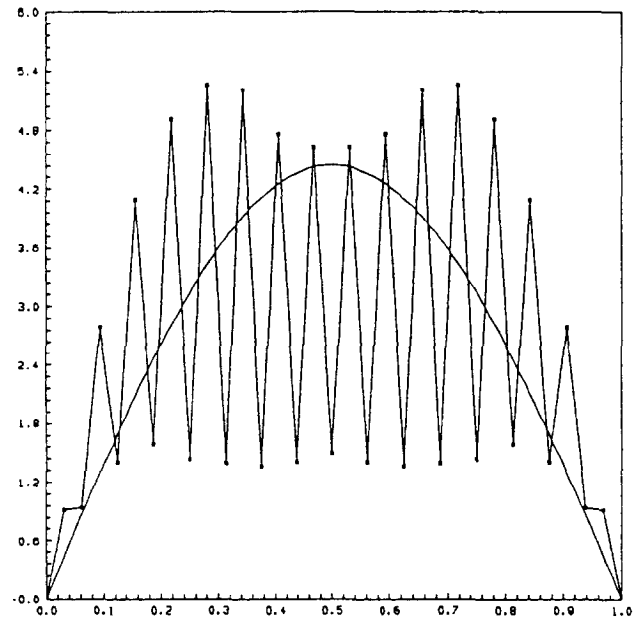

FIG. 3.9. Variations of $e^1(x_1, 0.5)$(—) and $e_c^1(x_1, 0.5)(\cdots)$ $(h = \frac{1}{32})$.

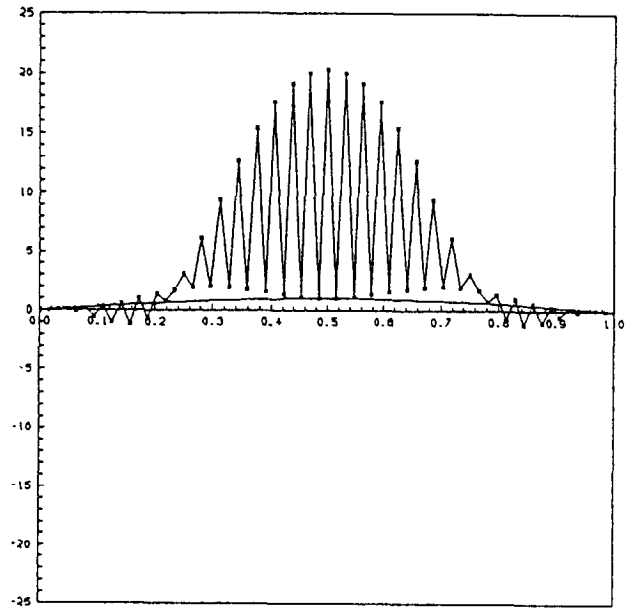

FIG. 3.11. Variations of $e^0(x_1, 0.5)$(—) and $e_c^0(x_1, 0.5)(\cdots)$ $(h = \frac{1}{64})$.

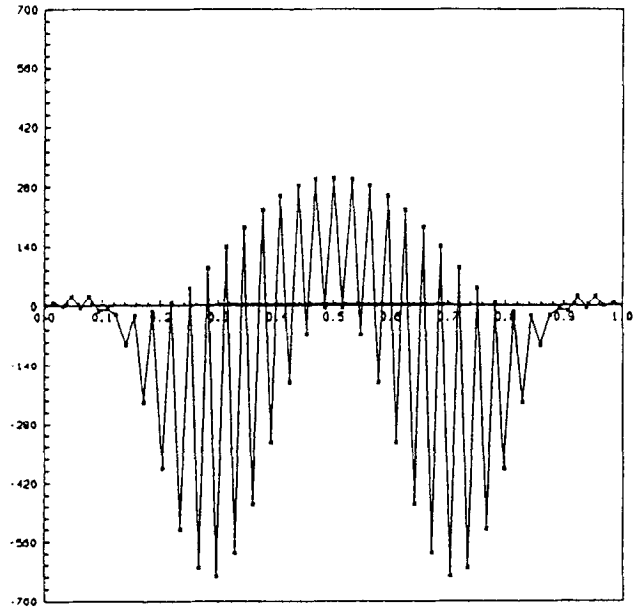

FIG. 3.12. Variations of $e^1(x_1, 0.5)$(—) and $e_c^1(x_1, 0.5)(\cdots)$ $(h = \frac{1}{64})$.

Consider now the particular situation, where

$$e_h^0 = w_{pq}, \qquad e_h^1 = 0. \tag{3.65}$$

Since the vectors w_{pq} are for $1 \leqslant p, q \leqslant I$, the *eigenvectors* of the discrete Laplace operator occurring in $(3.64)_1$ and that the corresponding eigenvalues $\lambda_{pq}(h)$ are given by

$$\lambda_{pq}(h) = \frac{4}{h^2}\left(\sin^2 p\pi\frac{h}{2} + \sin^2 q\pi\frac{h}{2}\right), \tag{3.66}$$

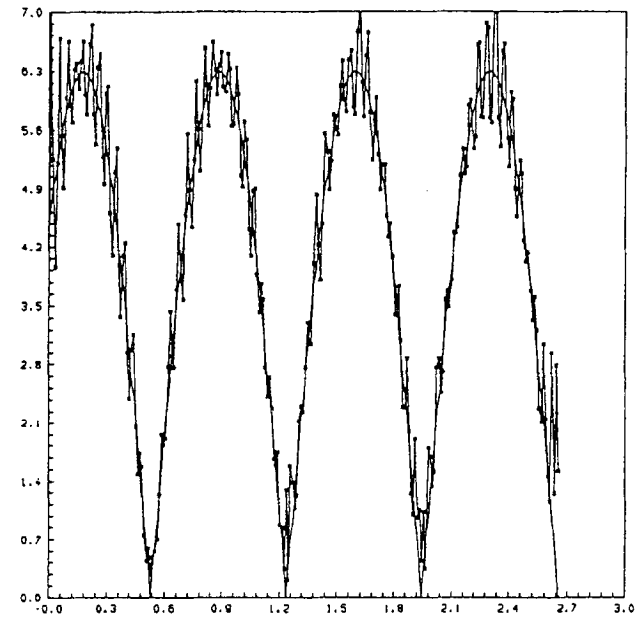

FIG. 3.13. Variations of $\|g(t)\|_{L^2(\Gamma)}$(—) and $\|g_c(t)\|_{L^2(\Gamma)}(\cdots)$ $(h = \frac{1}{64})$.

we can easily prove that the solution of (3.64), (3.65) is given by

$$\varphi_{ij}(t) = \sin p\pi ih \sin q\pi jh \cos(\sqrt{\lambda_{pq}(h)}\, t), \qquad 0 \leqslant i, j \leqslant I+1. \tag{3.67}$$

Next, we use (3.55) (see Section 3.6.3) to compute, from (3.67), the approximation of $\partial\varphi/\partial n$ at the boundary point $M_{0j} = \{0, jh\}$, with $1 \leqslant j \leqslant I$; thus, at time t, $\partial\varphi/\partial n$ is approximated at M_{0j} by

$$\delta\varphi_h(M_{0j}, t) = -\frac{1}{h}\sin p\pi h \sin q\pi jh \cos(\sqrt{\lambda_{pq}(h)}\, t). \tag{3.68}$$

If $1 \leqslant p \ll I$, the coefficient $K_h(p)$ defined by

$$K_h(p) = \frac{\sin p\pi h}{h} \tag{3.69}$$

is an approximation of $p\pi$ which is second-order accurate (with respect to h); now if $p \sim I/2$ we have $K_h(p) \sim I$, and if $p = I$ we have (since $h = 1/(I+1)$) $K_h(I) \sim \pi$.

Back to the *continuous problem*, it is quite clear that (3.64), (3.65) is in fact a semi-discrete approximation of the wave problem

$$\begin{aligned} &\Box\varphi = 0 \quad \text{in } Q, \qquad \varphi = 0 \quad \text{on } \Sigma \\ &\varphi(x, 0) = \sin p\pi x_1 \sin q\pi x_2, \qquad \varphi_t(x, 0) = 0. \end{aligned} \tag{3.70}$$

The solution of (3.70) is given by

$$\varphi(x, t) = \sin p\pi x_1 \sin q\pi x_2 \cos(\pi\sqrt{p^2+q^2}\, t). \tag{3.71}$$

Computing $(\partial\varphi/\partial n)|_\Sigma$ we obtain

$$\frac{\partial\varphi}{\partial n}(M_{0j}, t) = -p\pi \sin q\pi jh \cos(\pi\sqrt{p^2+q^2}\, t). \tag{3.72}$$

We observe that if $p \ll I$ and $q \ll I$, then $(\partial\varphi/\partial n)(M_{0j}, t)$ and $\delta\varphi_h(M_{0j}, t)$ are close quantities. Now, if the wave number is large, then the coefficient $K(p) = \pi p$ in (3.72) is much larger than the corresponding coefficient $K_h(p)$ in (3.68); we have actually

$$\frac{K(I/2)}{K_h(I/2)} \approx \frac{\pi}{2}, \qquad \frac{K(I)}{K_h(I)} \approx I.$$

Figure 2.2 of Section 2.5 still applies for the present situation (replace m by p) and shows that for $p, q > (I+1)/2$, the

approximate normal derivative operator introduces a very strong damping. We should have obtained similar results by considering, instead of (3.65), initial conditions such as

$$e_h^0 = 0, \qquad e_h^1 = w_{pq}. \tag{3.73}$$

From the above analysis it appears that the approximation of $(\partial\varphi/\partial n)|_\Sigma$, which is used to construct operator $\bigwedge_h^{\Delta t}$, introduces a very strong damping of the *large wave number components* of $\mathbf{e}_h$.

Possible cures for the ill-posedness of the discrete problem (3.59) have been discussed in [3, 4]. Reference [3], in particular, contains a detailed discussion of a *biharmonic Tychonoff regularization procedure*, where problem $\bigwedge \mathbf{e} = \mathbf{f}$ is approximated by a discrete version of

$$\varepsilon \mathbf{M} \mathbf{e}_\varepsilon + \bigwedge \mathbf{e}_\varepsilon = \mathbf{f} \qquad \text{in } \Omega, \tag{3.74}_1$$

$$\Delta e_\varepsilon^0 = e_\varepsilon^0 = e_\varepsilon^1 = 0 \qquad \text{on } \Gamma, \tag{3.74}_2$$

with $\mathbf{e}_\varepsilon = \{e_\varepsilon^0, e_\varepsilon^1\}$, and where, in (3.74), operator $\mathbf{M}$ is defined by $\mathbf{M} = \begin{pmatrix} \Delta & 0 \\ 0 & -\Delta \end{pmatrix}$.

Various theoretical and numerical issues associated to (3.74) are discussed in [3], including the choice of ε as a function of h; indeed elementary *boundary layer* considerations show that ε has to be of the order of h^2. The numerical results presented in [3, 4] validate convincingly the above regularization approach.

Also, in Ref. [3, p. 42], we suggest that *mixed finite element* approximations (see, e.g., [27] for an introduction to mixed finite element methods) may improve the quality of the numerical results; one of the reasons for this potential improvement is that mixed finite element methods are known to provide accurate approximations of derivatives and also that derivative values at selected nodes (including boundary ones) are natural degrees of freedom for these approximations. As shown in Ref. [28], this approach reduces substantially the unwanted oscillations, since *without* any regularization good numerical results have been obtained using mixed finite element implementations of HUM. The main drawback of this method is that (without regularization) the number of conjugate gradient iterations necessary to achieve convergence increases (slowly) with h (in fact, roughly, as $h^{-1/2}$); it seems, also, on the basis of numerical experiments, that the level of unwanted oscillations increases (slowly, again) with T.

Several other possible cures are listed in Ref. [3], except the obvious one, clearly suggested in the above reference by [3, p. 41, Fig. 9.1] (which is essentially our Fig. 2.2). This new (and simpler) cure consists of eliminating the *short wave length* components of $\mathbf{e}_h$ with wave numbers p and q larger than $(I+1)/2$; to achieve this radical filtering it suffices to define $\mathbf{e}_h$ on a finite difference grid of step size $\geqslant 2h$.

Justifying therefore the title of the present paper, this cure was inspired to us by the striking similarity between the damping mechanisms associated to the "naive" approximations of both the discrete Stokes problem and the present boundary control problem, and then by the way one can stabilize the Stokes problem, as shown in Section 2.5 (approach (a)). A *finite element* implementation of the above filtering technique is discussed in the following Section 3.9; also, for the calculations described in Section 4, we have defined $\mathbf{e}_h$ over a grid of step size $2h$.

3.9. A Finite Element Implementation of the Filtering Technique of Section 3.8

3.9.1. *Generalities*

A most natural fashion to combine HUM and the filtering technique discussed in Section 3.8 is to use *finite elements* for the space approximation; actually, as shown in Ref. [3, Section 6.2], special triangulations (like the one shown in Fig. 2.1) will give back finite difference approximations closely related to the one discussed in Section 3.6. For simplicity, we suppose that Ω is a polygonal domain of $\mathbb{R}^2$; we introduce then a triangulation $\mathcal{T}_h$ of Ω such that $\bar{\Omega} = \bigcup_{T \in \mathcal{T}_h} T$, with h the length of the largest edge(s) of $\mathcal{T}_h$. From $\mathcal{T}_h$, we define $\mathcal{T}_{h/2}$ by joining (see, again, Fig. 2.3), the midpoints of the edges of the triangles of $\mathcal{T}_h$. With P_1 the space of the polynomials in two variables of degree $\leqslant 1$, we define the spaces V_h and V_{0h} by

$$\begin{aligned} V_h &= \{v \mid v \in C^0(\bar{\Omega}),\ v|_T \in P_1,\ \forall T \in \mathcal{T}_h\}, \\ V_{0h} &= \{v \mid v \in V_h,\ v|_\Gamma = 0\}; \end{aligned} \tag{3.75}$$

similarly, we define $V_{h/2}$ and $V_{oh/2}$, by replacing h by $h/2$ in (3.75). We observe that $V_h \subset V_{h/2}$, $V_{0h} \subset V_{0h/2}$. We approximate then the $L^2(\Omega)$-scalar product over V_h by

$$(v, w)_h = \tfrac{1}{3} \sum_Q \omega_Q v(Q)\, w(Q), \qquad \forall v, w \in V_h, \tag{3.76}$$

where, in (3.76), Q describes the set of the vertices of $\mathcal{T}_h$ and where ω_Q is the area of the polygonal domain, union of those triangles of $\mathcal{T}_h$, with Q as a common vertex. Similarly, we define $(\cdot, \cdot)_{h/2}$ by substituting $h/2$ to h in (3.76).

3.9.2. *Approximation of* $\bigwedge \mathbf{e} = \mathbf{f}$

We approximate the fundamental equation $\bigwedge \mathbf{e} = \mathbf{f}$ by the following linear variational problem in $V_{0h} \times V_{0h}$:

$$\begin{aligned} &\mathbf{e}_h \in V_{0h} \times V_{0h}, \\ &\lambda_h^{\Delta t}(\mathbf{e}_h, \mathbf{v}) = \langle u^1, v^0 \rangle - \int_\Omega u^0 v^1 \, dx, \\ &\qquad \forall \mathbf{v} = \{v^0, v^1\} \in V_{0h} \times V_{0h}. \end{aligned} \tag{3.77}$$

In (3.77), $\langle \cdot, \cdot \rangle$ denotes the duality pairing between $H^{-1}(\Omega)$ and $H_0^1(\Omega)$, and the bilinear form $\lambda_h^{\Delta t}(\cdot, \cdot)$ is defined as follows

(i) Take $\mathbf{z}_h = \{z_h^0, z_h^1\} \in V_{0h} \times V_{0h}$ and solve, for $n = 0, ..., N$, the discrete wave equation

$$\begin{aligned} &\varphi_h^{n+1} \in V_{0h/2}, \\ &(\varphi_h^{n+1} + \varphi_h^{n-1} - 2\varphi_h^n, v)_{h/2} \\ &\quad + |\Delta t|^2 \int_\Omega \nabla \varphi_h^n \cdot \nabla v \, dx = 0, \quad \forall v \in V_{0h/2}, \end{aligned} \tag{3.78}$$

with the initial conditions

$$\varphi_h^0 = z_h^0, \qquad \varphi_h^1 - \varphi_h^{-1} = 2\Delta t \, z_h^1. \tag{3.79}$$

(ii) To approximate $\partial\varphi/\partial n$ over Σ, first introduce the complementary subspace $M_{h/2}$ of $V_{0h/2}$ in $V_{h/2}$ defined by

$$\begin{aligned} M_{h/2} = \{ &v \mid v \in V_{h/2}, v|_\Gamma = 0, \\ &\forall T \in \mathcal{T}_{h/2} \text{ such that } \partial T \cap \Gamma = \varnothing \}, \end{aligned} \tag{3.80}$$

and observe that $M_{h/2}$ is isomorphic to the space $\gamma V_{h/2}$ of the traces over Γ of the functions of $V_{h/2}$; the approximation of $(\partial\varphi/\partial n)|_\Gamma$ at $t = n\,\Delta t$ is then defined (cf. [3]) by solving the linear variational problem

$$\begin{aligned} &\delta\varphi_h^n \in \gamma V_{h/2}; \\ &\int_\Gamma \delta\varphi_h^n v \, d\Gamma = \int_\Omega \nabla \varphi_h^n \cdot \nabla v \, dx, \qquad \forall v \in M_{h/2}. \end{aligned} \tag{3.81}$$

Variants of (3.81), leading to linear systems with diagonal matrices are given in [3].

(iii) Now, for $n = N, N-1, ..., 0$, solve the discrete wave equation

$$\begin{aligned} &\psi_h^{n-1} \in V_{h/2}, \qquad \psi_h^{n-1} = \delta\varphi_h^{n-1} \qquad \text{on } \Gamma, \\ &(\psi_h^{n-1} + \psi_h^{n+1} - 2\psi_h^n, v)_{h/2} \\ &\quad + |\Delta t|^2 \int_\Omega \nabla \psi_h^n \cdot \nabla v \, dx = 0, \quad \forall v \in V_{0h/2}, \end{aligned} \tag{3.82}$$

initialized via

$$\psi_h^N = 0, \qquad \psi_h^{N+1} - \psi_h^{N-1} = 0. \tag{3.83}$$

(iv) Finally, define $\lambda_h^{\Delta t}(\cdot, \cdot)$ by

$$\begin{aligned} &\lambda_h^{\Delta t}(\mathbf{z}_h, \mathbf{v}) = (\lambda_h^0, v^0)_{h/2} + (\lambda_h^1, v^1)_{h/2}, \\ &\forall \mathbf{v} = \{v^0, v^1\} \in V_{0h} \times V_{0h}, \end{aligned} \tag{3.84}$$

where in (3.84), λ_h^0 and λ_h^1 belong both to $V_{0h/2}$ and satisfy

$$\begin{aligned} &\lambda_h^0(P) = \frac{\psi_h^1(P) - \psi_h^{-1}(P)}{2\Delta t}, \\ &\lambda_h^1(P) = -\psi_h^0(P), \qquad \forall P \text{ interior vertex of } \mathcal{T}_{h/2}. \end{aligned} \tag{3.85}$$

Following [3, Section 6] we can prove that

$$\begin{aligned} \lambda_h^{\Delta t}(\mathbf{e}_h, \check{\mathbf{e}}_h) = \Delta t \sum_{n=0}^{N} \alpha_n \int_\Gamma \delta\varphi_h^n \delta\check{\varphi}_h^n \, d\Gamma, \\ \forall \mathbf{e}_h, \check{\mathbf{e}}_h \in V_{0h} \times V_{0h}, \end{aligned} \tag{3.86}$$

where, in (3.86), $\alpha_0 = \alpha_N = \frac{1}{2}$ and $\alpha_n = 1$ if $0 < n < N$.

It follows from (3.86) that $\lambda_h^{\Delta t}(\cdot, \cdot)$ is *symmetric* and *positive semi-definite*. As in [3, Section 6.2], we should prove that $\lambda_h^{\Delta t}(\cdot, \cdot)$ is *positive definite* if T is sufficiently large and if Ω is a square (or a rectangle) and $\mathcal{T}_h$, $\mathcal{T}_{h/2}$ *regular triangulations* of Ω. From the properties of $\lambda_h^{\Delta t}(\cdot, \cdot)$ the linear variational problem (3.77) (which approximates $\bigwedge \mathbf{e} = \mathbf{f}$) can be solved by a *conjugate gradient algorithm* operating in $V_{0h} \times V_{0h}$. This algorithm is described in Section 3.9.3.

3.9.3. *Conjugate Gradient Solution of the Approximate Problem* (3.77)

The conjugate gradient algorithm for solving problem (3.77) is a finite element implementation of algorithm (3.30)–(3.46) (see Section 3.5.2); it is also a simple variant of algorithm (6.22)–(6.44) described in [3, Section 6.3].

DESCRIPTION OF THE CONJUGATE GRADIENT ALGORITHM.

Step 0. *Initialization.*

$$e_0^0 \in V_{0h}, \qquad e_0^1 \in V_{0h} \qquad \text{are given;} \tag{3.87}$$

solve then, for $n = 0, 1, ..., N$, the discrete forward wave equation

$$\begin{aligned} &\left(\frac{\varphi_0^{n+1} + \varphi_0^{n-1} - 2\varphi_0^n}{|\Delta t|^2}, v \right)_{h/2} \\ &\quad + \int_\Omega \nabla \varphi_0^n \cdot \nabla v \, dx = 0, \\ &\quad \forall v \in V_{0h/2}; \varphi_0^{n+1} \in V_{0h/2}, \end{aligned} \tag{3.88}$$

initialized by

$$\varphi_0^0 = e_0^0, \qquad \varphi_0^1 - \varphi_0^{-1} = 2\Delta t \, e_0^1, \tag{3.89}$$

and store φ_0^N, φ_0^{N+1}.

Then for $n=N, N-1, ..., 0$, compute φ_0^n, $\delta\varphi_0^n$, ψ_0^{n-1} by backward (discrete) time integration, as follows:

(i) If $n=N$ compute $\delta\varphi_0^N$ from φ_0^N using (3.81).
If $n<N$, compute first φ_0^n by solving

$$\left(\frac{\varphi_0^n+\varphi_0^{n+2}-2\varphi_0^{n+1}}{|\Delta t|^2}, v\right)_{h/2} + \int_\Omega \nabla\varphi_0^{n+1}\cdot\nabla v\, dx = 0, \quad \forall v\in V_{0h/2};\ \varphi_0^n\in V_{0h/2}, \tag{3.90}$$

and then $\delta\varphi_0^n$ by using (3.81).

(ii) Take $\psi_0^n=\delta\varphi_0^n$ on Γ and use

$$\left(\frac{\psi_0^{n-1}+\psi_0^{n+1}-2\psi_0^n}{|\Delta t|^2}, v\right)_{h/2} + \int_\Omega \nabla\psi_0^n\cdot\nabla v\, dx = 0, \quad \forall v\in V_{0h/2}, \tag{3.91}$$

to compute the values taken by $\psi_0^{n-1}(\in V_{h/2})$ at the interior vertices of $\mathcal{T}_{h/2}$. These calculations are initialized by

$$\psi_0^N(P)=0, \qquad (\psi_0^{N+1}-\psi_0^{N-1})(P)=0, \quad \forall P \text{ interior vertex of } \mathcal{T}_{h/2}. \tag{3.92}$$

Compute then $\mathbf{g}_0=\{g_0^0, g_0^1\}\in V_{0h}\times V_{0h}$ by solving the discrete Dirichlet problem

$$g_0^0\in V_{0h}, \quad \int_\Omega \nabla g_0^0\cdot\nabla v\, dx = \left(\frac{\psi_0^1-\psi_0^{-1}}{2\Delta t}, v\right)_{h/2} - \langle u^1, v\rangle, \quad \forall v\in V_{0h}, \tag{3.93}$$

and then

$$g_0^1\in V_{0h}, \quad (g_0^1, v)_h = \int_\Omega u^0 v\, dx - (\psi_0^0, v)_{h/2}, \quad \forall v\in V_{0h}. \tag{3.94}$$

If $\mathbf{g}_0=0$, or is small, take $\mathbf{e}_h=\mathbf{e}_0$; if not set

$$\mathbf{w}_0=\mathbf{g}_0. \tag{3.95}$$

Then, for $k\geqslant 0$, assuming that $\mathbf{e}_k$, $\mathbf{g}_k$, $\mathbf{w}_k$, φ_k, ψ_k are known, compute $\mathbf{e}_{k+1}$, $\mathbf{g}_{k+1}$, $\mathbf{w}_{k+1}$, φ_{k+1}, ψ_{k+1} as follows:

Step 1. *Descent.* For $n=0, 1, ..., N$, solve the discrete forward wave equation

$$\left(\frac{\bar\varphi_k^{n+1}+\bar\varphi_k^{n-1}-2\bar\varphi_k^n}{|\Delta t|^2}, v\right)_{h/2} + \int_\Omega \nabla\bar\varphi_k^n\cdot\nabla v\, dx = 0, \quad \forall v\in V_{0h/2};\ \bar\varphi_k^{n+1}\in V_{0h/2}, \tag{3.96}$$

initialized by

$$\bar\varphi_k^0=w_k^0, \qquad \bar\varphi_k^1-\bar\varphi_k^{-1}=2\Delta t\, w_k^1, \tag{3.97}$$

and store $\bar\varphi_k^N$, $\bar\varphi_k^{N+1}$.

Then for $n=N, N-1, ..., 0$, compute $\bar\varphi_k^n$, $\delta\bar\varphi_k^n$, $\bar\psi_k^{n-1}$ by backward time integration as follows:

(i) If $n=N$, compute $\delta\bar\varphi_k^N$ from $\bar\varphi_k^N$ using (3.81).
If $n<N$, compute first $\bar\varphi_k^n$ by solving

$$\left(\frac{\bar\varphi_k^n+\bar\varphi_k^{n+2}-2\bar\varphi_k^{n+1}}{|\Delta t|^2}, v\right)_{h/2} + \int_\Omega \nabla\bar\varphi_k^{n+1}\cdot\nabla v\, dx = 0, \quad \forall v\in V_{0h/2};\ \bar\varphi_k^n\in V_{0h/2}, \tag{3.98}$$

and then $\delta\bar\varphi_k^n$ by using (3.81).

(ii) Take $\bar\psi_k^n=\delta\bar\varphi_k^n$ on Γ and use

$$\left(\frac{\bar\psi_k^{n-1}+\bar\psi_k^{n+1}-2\bar\psi_k^n}{|\Delta t|^2}, v\right)_{h/2} + \int_\Omega \nabla\bar\psi_k^n\cdot\nabla v\, dx = 0, \quad \forall v\in V_{0h/2}, \tag{3.99}$$

to compute the values taken by $\bar\psi_k^{n-1}(\in V_{h/2})$ at the interior vertices of $\mathcal{T}_{h/2}$. These calculations are initialized by

$$(\bar\psi_k^{N+1}-\bar\psi_k^{N-1})(P) = \bar\psi_k^N(P)=0, \quad \forall P \text{ interior vertex of } \mathcal{T}_{h/2}. \tag{3.100}$$

Compute now $\bar{\mathbf{g}}_k(=\{\bar g_k^0, \bar g_k^1\})\in V_{0h}\times V_{0h}$ by

$$\bar g_k^0\in V_{0h}, \quad \int_\Omega \nabla\bar g_k^0\cdot\nabla v\, dx = \left(\frac{\bar\psi_k^1-\bar\psi_k^{-1}}{2\Delta t}, v\right)_{h/2}, \quad \forall v\in V_{0h}, \tag{3.101}$$

$$\bar g_k^1\in V_{0h}, \quad (\bar g_k^1, v)_h = -(\bar\psi_k^0, v)_{h/2}, \quad \forall v\in V_{0h}, \tag{3.102}$$

and then ρ_k by

$$\rho_k = \frac{\int_\Omega |\nabla g_k^0|^2\, dx + (g_k^1, g_k^1)_h}{\int_\Omega \nabla\bar g_k^0\cdot\nabla w_k^0\, dx + (\bar g_k^1, w_k^1)_h}. \tag{3.103}$$

Once ρ_k is known, compute

$$\mathbf{e}_{k+1} = \mathbf{e}_k - \rho_k \mathbf{w}_k, \tag{3.104}$$

$$\varphi_{k+1} = \varphi_k - \rho_k \bar{\varphi}_k, \tag{3.105}$$

$$\psi_{k+1} = \psi_k - \rho_k \bar{\psi}_k, \tag{3.106}$$

$$\mathbf{g}_{k+1} = \mathbf{g}_k - \rho_k \bar{\mathbf{g}}_k. \tag{3.107}$$

Step 2. Test of the convergence and construction of the new descent direction. If $\mathbf{g}_{k+1} = 0$, or is small, take $\mathbf{e}_h = \mathbf{e}_{k+1}$, $\varphi_h = \varphi_{k+1}$, $\psi_h = \psi_{k+1}$; if not, compute

$$\gamma_k = \frac{\int_\Omega |\nabla g^0_{k+1}|^2\, dx + (g^1_{k+1}, g^1_{k+1})_h}{\int_\Omega |\nabla g^0_k|^2\, dx + (g^1_k, g^1_k)_h}, \tag{3.108}$$

and set

$$\mathbf{w}_{k+1} = \mathbf{g}_{k+1} + \gamma_k \mathbf{w}_k. \tag{3.109}$$

Do $k = k+1$ and go to (3.96).

Remark 3.6. The above algorithm may seem a little bit complicated at first glance (23 statements); in fact, it is fairly easy to implement, since the only non-trivial part of it is the solution (on the coarse grid) of the discrete Dirichlet problems (3.93) and (3.101). An interesting feature of algorithm (3.87)–(3.109) is that the backward integration of the discrete wave equations (3.88) and (3.96) provides a very substantial computer memory saving. To illustrate this claim, let us consider the case where $\Omega = (0,1)\times(0,1)$, $T = 2\sqrt{2}$, $h = \frac{1}{64}$, $\Delta t = h/2\sqrt{2} = \sqrt{2}/256$; we have then—approximately—$(512)^2$ discretization points on Σ, therefore in that specific case, using algorithm (3.87)–(3.109) avoids the storage of 2.62×10^5 real numbers. The saving would be even more substantial for larger T and would be an absolute necessity for three-dimensional problems.

Remark 3.7. The above remark also shows the interest of the HUM approach from a computational point of view. In the original control problem, the unknown is the control g which is defined over Σ; using HUM, the unknown is then the solution $\mathbf{e}$ of $\Lambda\, \mathbf{e} = \mathbf{f}$. If one considers again the particular case of Remark 3.6, i.e., $\Omega = (0,1)\times(0,1)$, $T = 2\sqrt{2}$, $h = \frac{1}{64}$, $\Delta t = h/2\sqrt{2}$, the unknown g will be approximated by a finite dimensional vector with 2.62×10^5 components, while $\mathbf{e}$ is approximated by $\mathbf{e}_h$ of dimension $2 \times (63)^2 = 7.938 \times 10^3$, a substantial memory saving indeed. Numerical results obtained using algorithm (3.87)–(3.109) will be discussed in Section 4.

4. EXPERIMENTAL VALIDATION OF THE FILTERING PROCEDURE OF SECTION 3.9 VIA THE SOLUTION OF THE TEST PROBLEM OF SECTION 3.7

We consider in this section the solution of the test problem of Section 3.7. The filtering technique discussed in Section 3.9 is applied with $\mathcal{T}_h$ a regular triangulation like the one shown in Fig. 2.1; we recall that $\mathcal{T}_h$ is used to approximate $\mathbf{e}_h$, while φ and ψ are approximated on $\mathcal{T}_{h/2}$ as shown in Section 3.9. Instead of taking h to be equal to the length of the largest edges of $\mathcal{T}_h$, it is convenient here to take h as the length of the edges adjacent to the right angles of $\mathcal{T}_h$. The approximate problems (3.77) have been solved by the conjugate gradient algorithm (3.87)–(3.109) of Section 3.9.3. This algorithm has been *initialized* with $e^0_0 = e^1_0 = 0$ and we have used

$$\frac{\int_\Omega |\nabla g^0_k|^2\, dx + (g^1_k, g^1_k)_h}{\int_\Omega |\nabla g^0_0|^2\, dx + (g^1_0, g^1_0)_h} \leqslant 10^{-14} \tag{4.1}$$

as *stopping criterium* (for calculations on a CRAY X-MP).

Let us mention also that the functions u^0, u^1, g of the test problem of Section 3.7, satisfy

$$\|u^0\|_{L^2(\Omega)} = 12{,}92\cdot\ldots, \qquad \|u^1\|_{H^{-1}(\Omega)} = 11.77\ldots,$$
$$\|g\|_{L^2(\Sigma)} = 7.38668\ldots.$$

In the sequel, we shall denote by $\|\cdot\|_{0,\Omega}$, $|\cdot|_{1,\Omega}$, $\|\cdot\|_{-1,\Omega}$, $\|\cdot\|_{0,\Sigma}$ the $L^2(\Omega)$, $H^1_0(\Omega)$, $H^{-1}(\Omega)$, $L^2(\Sigma)$ norms, respectively (here $|v|_{1,\Omega} = (\int_\Omega |\nabla v|^2\, dx)^{1/2}$ and $\|v\|_{-1,\Omega} = |w|_{1,\Omega}$, where $w \in H^1_0(\Omega)$ is the solution of the Dirichlet problem $-\Delta w = v$ in Ω, $w = 0$ on Γ).

To approximate problem $\Lambda\, \mathbf{e} = \mathbf{f}$ by the discrete problem (3.77) we have been using $h = \frac{1}{4}, \frac{1}{8}, \frac{1}{16}, \frac{1}{32}, \frac{1}{64}$ and $\Delta t = h/2\sqrt{2}$ (since the wave equations are solved on a space/time grid of step size $h/2$ for the space discretization and $h/2\sqrt{2}$ for the time discretization); we recall that $T = 15/4\sqrt{2}$.

Results of our numerical experiments have been summarized in Table II. In this table, e^0_c, e^1_c, g_c are defined as in Section 3.7, and the new quantities u^0_c, u^1_c are the discrete analogues of $-\psi(0)$ and $(\partial\psi/\partial t)(0)$, where ψ is the solution of (3.6), associated via (3.5), to the solution $\mathbf{e}$ of $\Lambda\, \mathbf{e} = \mathbf{f}$.

Comparing the above results to those in Table I, the following facts appear quite clearly

(i) The filtering method described in Section 3.9 has been a very effective cure to the ill-posedness of the approximate problem (3.59).

(ii) The number of conjugate gradient iterations necessary to achieve the convergence is (for h sufficiently small) essentially independent of h; in fact, if one realizes that for $h = \frac{1}{64}$ the number of unknowns is $2 \times (63)^2 = 7938$, converging in 12 iterations is a fairly good performance.

The results of Table II compare favorably with those displayed in Tables 10.3 and 10.4 of [3, pp. 58, 59] which were obtained using the Tychonoff regularization procedure briefly recalled in Section 3.8; in fact fewer iterations are needed here, implying a smaller CPU time (actually the

TABLE II

$\Delta t = h/2\sqrt{2}$

$h/2$	1/8	1/16	1/32	1/64	1/128
Number of conjugate gradient iterations	7	10	12	12	12
CPU time (s) CRAY X-MP	0.1	0.6	2.8	14.8	83.9
$\frac{\|e^0 - e_c^0\|_{0,\Omega}}{\|e^0\|_{0,\Omega}}$	9.6×10^{-2}	2.6×10^{-2}	2.2×10^{-2}	6.4×10^{-3}	1.5×10^{-3}
$\frac{\|e^0 - e_c^0\|_{1,\Omega}}{\|e^0\|_{1,\Omega}}$	3.5×10^{-1}	1.8×10^{-1}	9×10^{-2}	4.4×10^{-2}	2.2×10^{-2}
$\frac{\|e^1 - e_c^1\|_{0,\Omega}}{\|e^1\|_{0,\Omega}}$	1×10^{-1}	2.6×10^{-2}	1.5×10^{-2}	7×10^{-3}	3.2×10^{-3}
$\frac{\|u^0 - u_c^0\|_{0,\Omega}}{\|u^0\|_{0,\Omega}}$	2.4×10^{-8}	3×10^{-8}	6×10^{-8}	8.3×10^{-8}	6.6×10^{-8}
$\frac{\|u^1 - u_c^1\|_{-1,\Omega}}{\|u^1\|_{-1,\Omega}}$	6.9×10^{-7}	4.6×10^{-7}	9.4×10^{-6}	2×10^{-5}	8.5×10^{-5}
$\frac{\|g - g_c\|_{0,\Sigma}}{\|g\|_{0,\Sigma}}$	1.2×10^{-1}	4.3×10^{-2}	2×10^{-2}	7.6×10^{-3}	3.4×10^{-3}
$\|g_c\|_{0,\Sigma}$	7.271	7.386	7.453	7.405	7.381

Note. We take $h/2$ as the discretization parameter to make easier comparisons with the results of Table 3I and of [2, Section 10]).

CPU time seems to be a *sublinear* function of h^{-3} which is within to a multiplicative constant of the number of points of the space/time discretization grid). Table II also shows that the approximation errors (roughly) satisfy

$$\|e^0 - e_c^0\|_{L^2(\Omega)} = O(h^2), \qquad \|e^0 - e_c^0\|_{H_0^1(\Omega)} = O(h), \tag{4.2}_1$$

$$\|e^1 - e_c^1\|_{L^2(\Omega)} = O(h), \tag{4.2}_2$$

$$\|g - g_c\|_{L^2(\Sigma)} = O(h). \tag{4.2}_3$$

Estimates $(4.2)_1$ and $(4.2)_2$ are of optimal order with respect to h in the sense that they have the order that we can expect when one approximates the solution of a boundary value problem, for a second-order elliptic operator, by piecewise linear finite element approximations; this result is not surprising since (from Section 3.4.2, relation (3.12)) the operator $\wedge$ associated to $\Omega = (0, 1) \times (0, 1)$ behaves, *for T sufficiently large*, like

$$2T \begin{pmatrix} -\Delta & 0 \\ 0 & I \end{pmatrix} \tag{4.3}$$

(we have here $x_0 = (0.5, 0.5)$ and $C = 0.5$).

In order to visualize the influence of h we have plotted for $h = \frac{1}{4}, \frac{1}{8}, \frac{1}{16}, \frac{1}{32}, \frac{1}{64}$, and $\Delta t = h/2\sqrt{2}$ the exact solutions e^0, e^1, g and the corresponding computed solutions e_c^0, e_c^1, g_c. To be more precise, we have shown the graphs of the functions $x_1 \to e^0\ (x_1, 0.5)$, $x_1 \to e^1\ (x_1, 0.5)$, $t \to \|g(t)\|_{L^2(\Sigma)}$ (solid lines) and of the corresponding computed functions (dotted lines). These results have been reported on Figs. 4.1 to 4.5, and the captions there are self-explanatory.

The above numerical experiments have been done with $T = 15/4\sqrt{2}$; in order to study the influence of T we have kept u^0 and u^1 as in the above numerical experiments and taken $T = 28.2843$. For $h = \frac{1}{64}$ and $\Delta t = h/2\sqrt{2}$ we need just 10 iterations of algorithm (3.87)–(3.110) to achieve convergence, the corresponding CRAY X-MP CPU time being then 800 s (!) (the number of grid points for the space/time discretization is now $\sim 86 \times 10^6$). We have $\|g_c\|_{L^2(\Sigma)} = 2.32$, $\|u^0 - u_c^0\|_{L^2(\Omega)} = 5.8 \times 10^{-6}$, and $\|u^1 - u_c^1\|_{-1,\Omega} = 1.6 \times 10^{-5}$. The most interesting results are the ones reported on Figs. 4.6a and b. There, we have compared Te_c^0 and Te_c^1 (for $T = 28.2843$) to the corresponding theoretical limits χ^0 and χ^1 which, according to Section 3.4.2, relations (3.13)–(3.15), are given by

$$-\Delta\chi^0 = u^1/2 \quad \text{in } \Omega, \qquad \chi^0 = 0 \quad \text{on } \Gamma, \tag{4.4}$$

$$\chi^1 = -u^0/2. \tag{4.5}$$

The *solid* curves represent the variations of $x_1 \to \chi^0(x_1, 0.5)$ and of $x_1 \to \chi^1(x_1, 0.5)$, while the *dotted* curves represent the variations of $x_1 \to Te_c^0(x_1, 0.5)$ and $x_1 \to Te_c^1(x_1, 0.5)$. In our opinion the above figures provide an excellent *numerical verification* of the convergence result (3.13) of Section 3.4.2 (we observe at $x_1 = 0$ and $x_1 = 1$ a (numerical) *Gibbs phenomenon* associated to the L^2 convergence of Te_c^1 to χ^1). Conversely, these results provide a *validation* of the

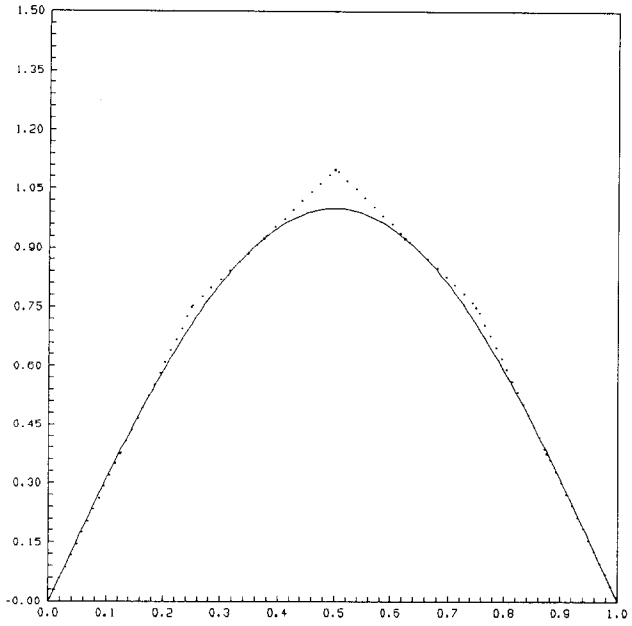

(a)

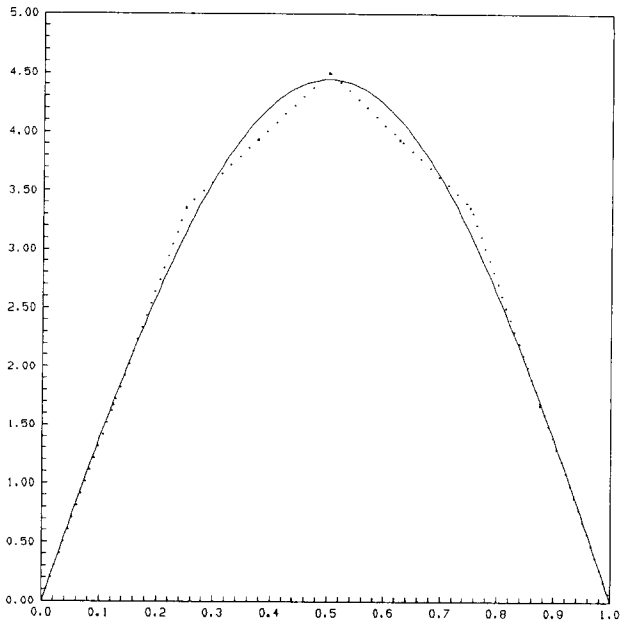

(b)

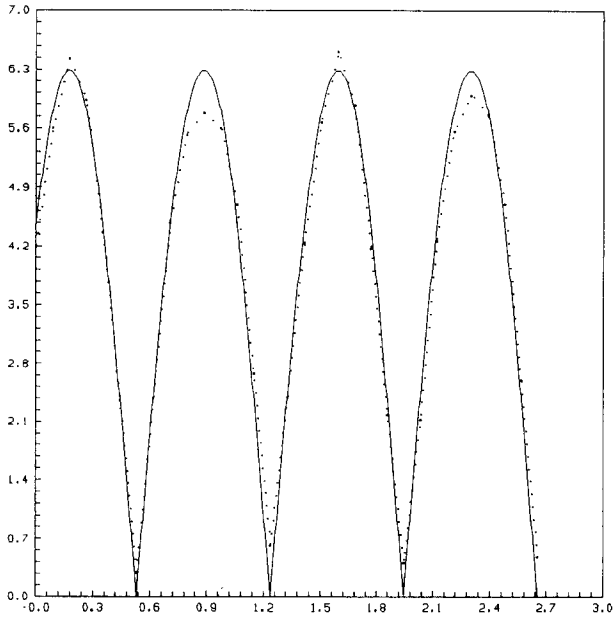

(c)

FIG. 4.1. ($h=\frac{1}{4}$, $\Delta t=h/2\sqrt{2}$): (a) Variation of $e^0(x_1, 0.5)$(—) and $e_c^0(x_1, 0.5)(\cdots)$; (b) Variation of $e^1(x_1, 0.5)$(—) and $e_c^1(x_1, 0.5)(\cdots)$; (c) Variation of $\|g\|_{L^2(\Gamma)}$(—) and $\|g_c\|_{L^2(\Gamma)}(\cdots)$.

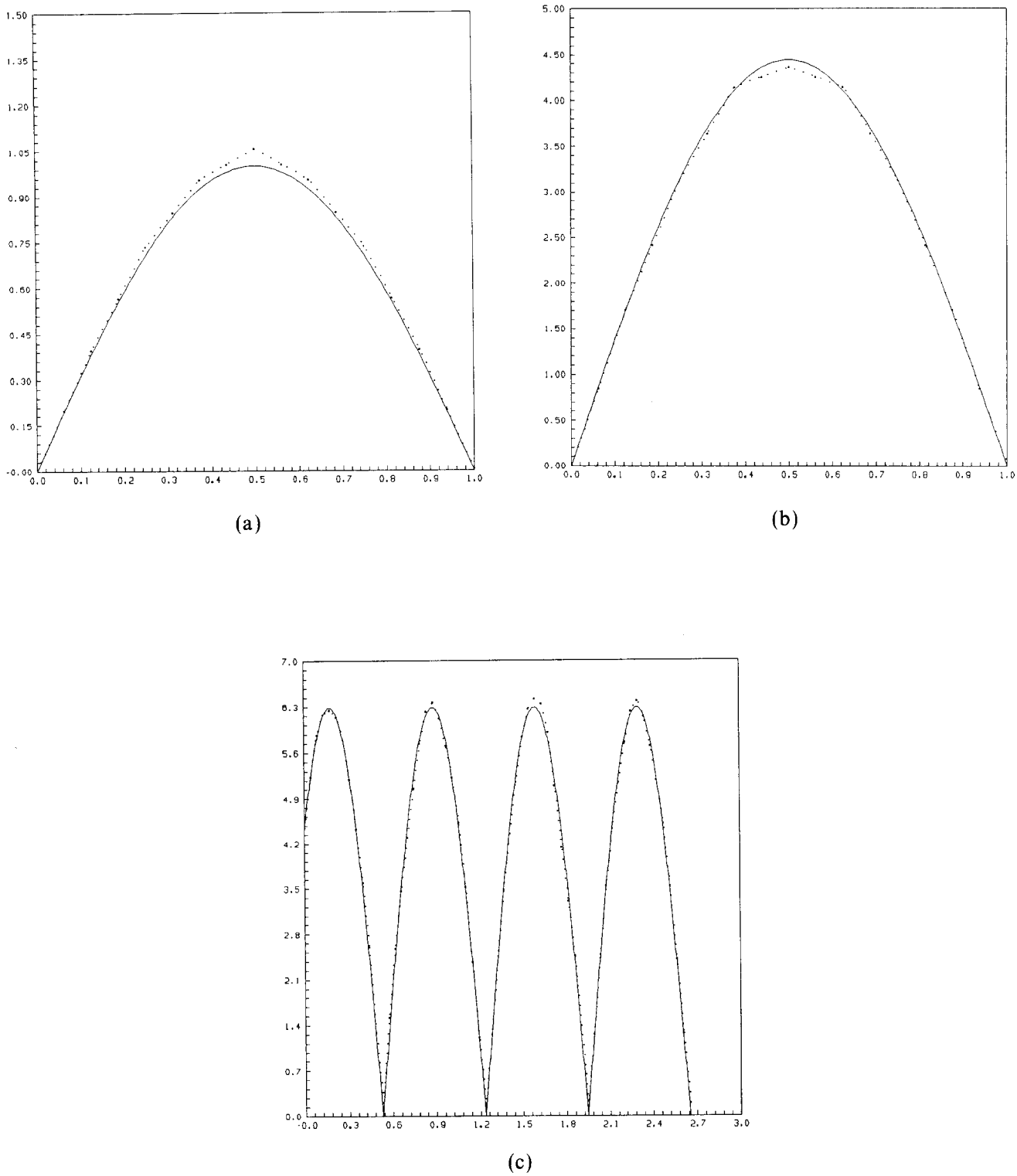

FIG. 4.2. ($h=\frac{1}{8}$, $\Delta t=h/2\sqrt{2}$): (a) Variation of $e^0(x_1, 0.5)$(—) and $e_c^0(x_1, 0.5)(\cdots)$; (b) Variation of $e^1(x_1, 0.5)$(—) and $e_c^1(x_1, 0.5)(\cdots)$; (c) Variation of $\|g\|_{L^2(\Gamma)}$(—) and $\|g_c\|_{L^2(\Gamma)}(\cdots)$.

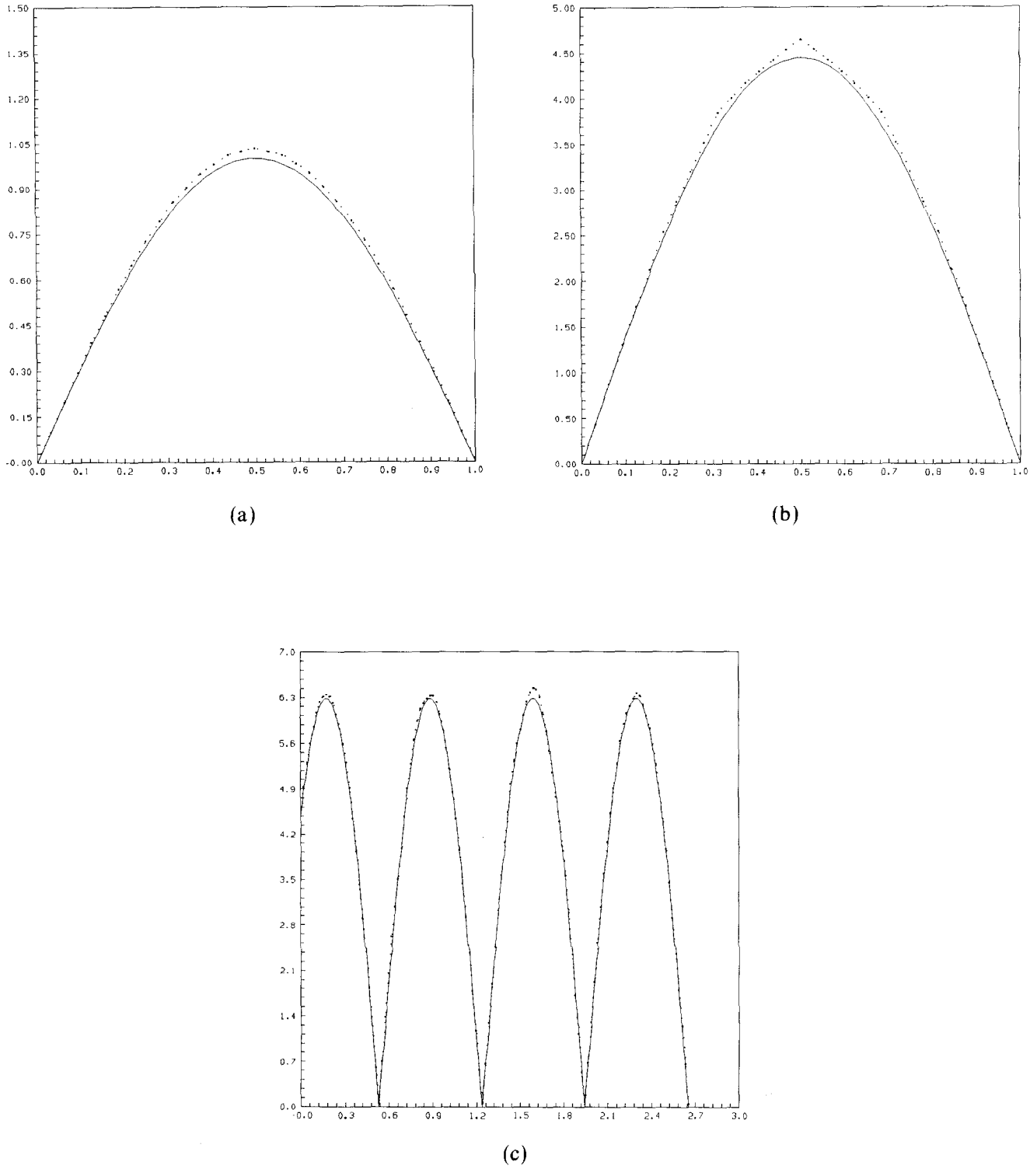

FIG. 4.3. ($h = \frac{1}{16}$, $\Delta t = h/2\sqrt{2}$): (a) Variation of $e^0(x_1, 0.5)$(—) and $e_c^0(x_1, 0.5)(\cdots)$; (b) Variation of $e^1(x_1, 0.5)$(—) and $e_c^1(x_1, 0.5)(\cdots)$; (c) Variation of $\|g\|_{L^2(\Gamma)}$(—) and $\|g_c\|_{L^2(\Gamma)}(\cdots)$.

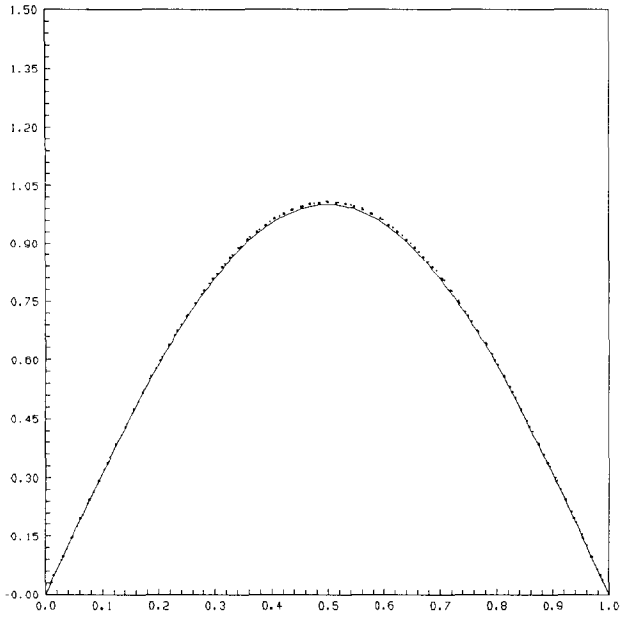

(a)

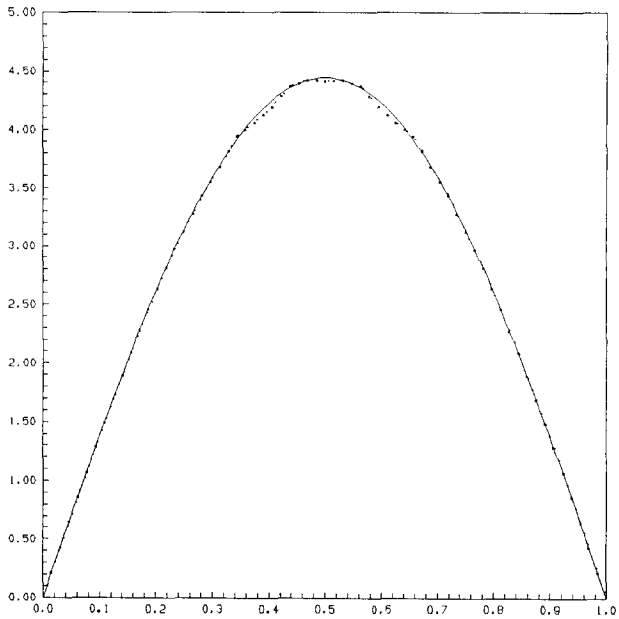

(b)

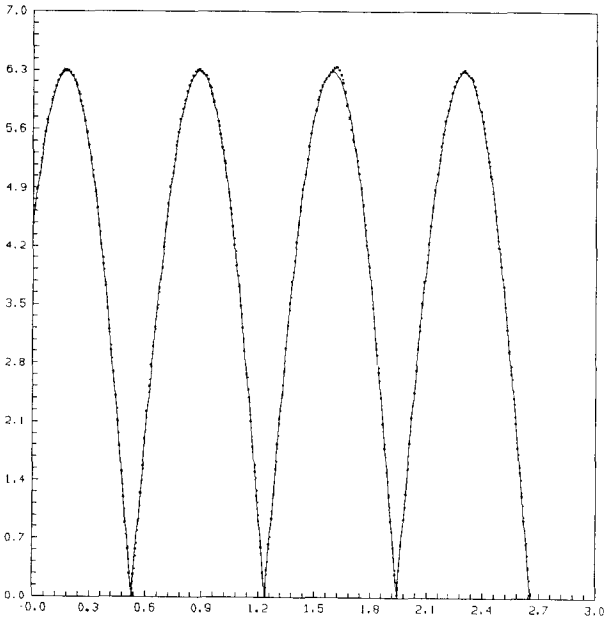

(c)

FIG. 4.4. ($h=\frac{1}{32}$, $\Delta t=h/2\sqrt{2}$): (a) Variation of $e^0(x_1, 0.5)$(—) and $e_c^0(x_1, 0.5)(\cdots)$; (b) Variation of $e^1(x_1, 0.5)$(—) and $e_c^1(x_1, 0.5)(\cdots)$; (c) Variation of $\|g\|_{L^2(\Gamma)}$(—) and $\|g_c\|_{L^2(\Gamma)}(\cdots)$.

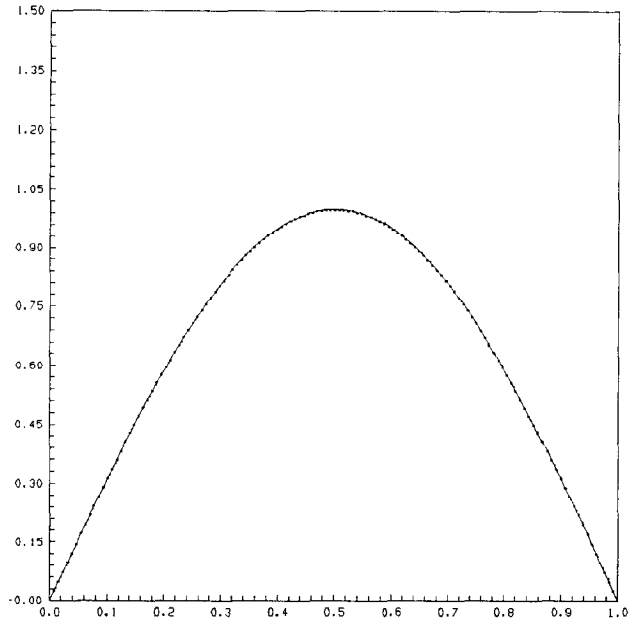

(a)

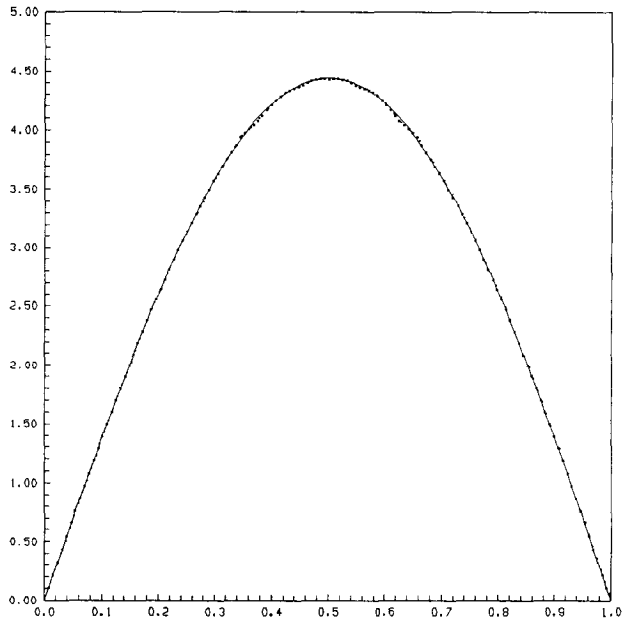

(b)

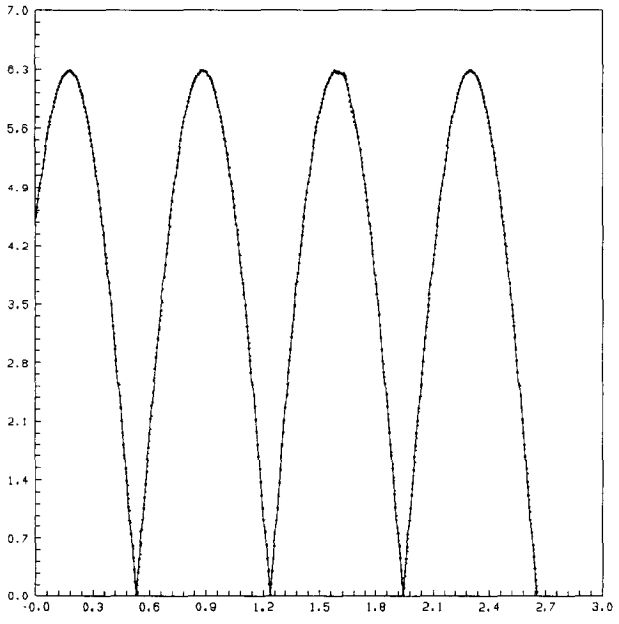

(c)

FIG. 4.5. ($h = \frac{1}{64}$, $\Delta t = h/2\sqrt{2}$): (a) Variation of $e^0(x_1, 0.5)$(—) and $e_c^0(x_1, 0.5)(\cdots)$; (b) Variation of $e^1(x_1, 0.5)$(—) and $e_c^1(x_1, 0.5)(\cdots)$; (c) Variation of $\|g\|_{L^2(\Gamma)}$(—) and $\|g_c\|_{L^2(\Gamma)}(\cdots)$.

numerical methodology discussed here; they show that this methodology is particularly robust, accurate, non-dissipative and perfectly able to handle very long time intervals $[0, T]$. Actually, it will be shown in [29] that the above-mentioned qualities of our numerical methods persist for initial data u^0 and u^1 much rougher than those considered in Sections 3.7 of the present article.

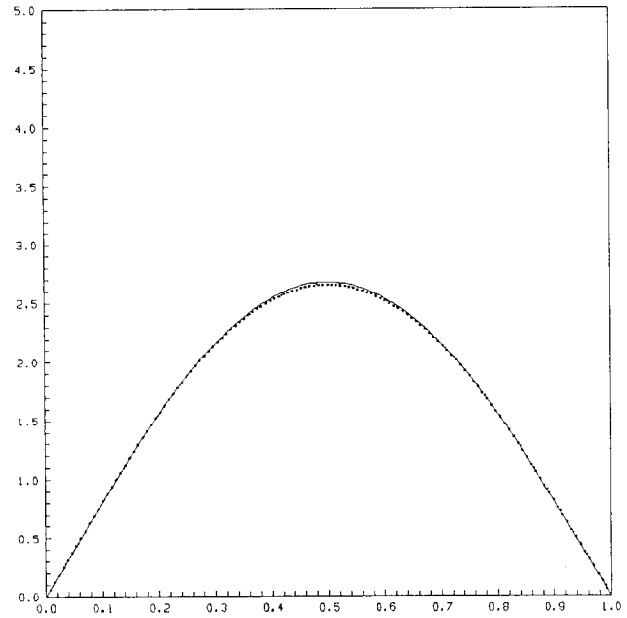

(a)

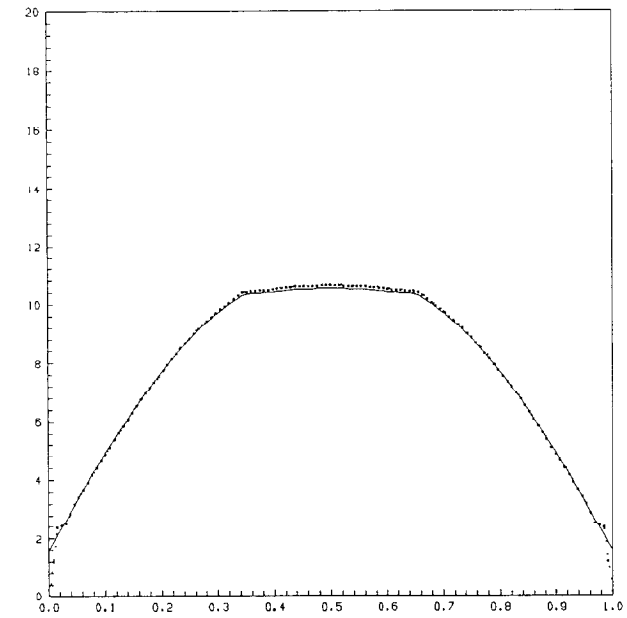

(b)

FIG. 4.6. ($h=\frac{1}{64}$, $\Delta t=h/2\sqrt{2}$, $T=28.2843$): (a) Variation of $\chi^0(x_1, 0.5)$(—) and $Te_c^0(x_1, 0.5)(\cdots)$; (b) Variation of $\chi^1(x_1, 0.5)$(—) and $Te_c^1(x_1, 0.5)(\cdots)$.

5. SOME COMMENTS ON THE WAVELET APPROXIMATION OF THE NAVIER–STOKES EQUATIONS

5.1. Synopsis

The main goal of this section is to briefly discuss some issues associated to the *wavelet approximation of the incompressible Navier–Stokes equations*

$$\frac{\partial \mathbf{u}}{\partial t} - \nu \nabla^2 \mathbf{u} + (\mathbf{u} \cdot \nabla)\mathbf{u} + \nabla p = \mathbf{f} \qquad \text{in } \Omega, \tag{5.1}$$

$$\nabla \cdot \mathbf{u} = 0 \qquad \text{in } \Omega, \tag{5.2}$$

completed with appropriate *initial* and *boundary conditions*; notation is like in Section 2, with the *nonlinear* term in (5.1) defined by

$$(\mathbf{u} \cdot \nabla)\mathbf{u} = \left\{ \sum_{j=1}^{d} u_j \frac{\partial u_i}{\partial x_j} \right\}_{i=1}^{d}.$$

Wavelets have become a generic name denoting various mathematical objects: the wavelets that we have in mind are the *compactly supported* ones introduced by I. Daubechies in [30], motivated by *signal processing* applications. Indeed, it has been shown in [31, 32] that the Daubechies wavelets have interesting possibilities concerning the numerical solution of *partial differential equations*, including the *viscous Burgers equation*

$$u_t + uu_x = \nu u_{xx},$$

where the viscosity ν is small; the main difficulty with Daubechies wavelets is the treatment of boundary conditions, particularly for domains with a complicated shape.

5.2. Generalities on Compactly Supported Wavelets

As mentioned just above, the *wavelets* that we consider are the *compactly supported* ones introduced by I. Daubechies in [30]. These wavelet functions are defined from a so-called *scaling function* φ solution of the *scaling relation*:

$$\varphi(x) = \sum_{k=0}^{2N-1} a_k \varphi(2x - k), \qquad \forall x \in \mathbb{R}. \tag{5.3}$$

If we require the scaling function φ to satisfy, for example,

$$\int_{\mathbb{R}} \varphi(x)\, dx = 1, \tag{5.4}$$

then relation (5.3) clearly implies that

$$\sum_{k=0}^{2N-1} a_k = 2. \tag{5.5}$$

If we require now the *translates* of φ by the integers to be *orthogonal*, i.e., to satisfy

$$\int_{\mathbb{R}} \varphi(x-l)\,\varphi(x-m)\,dx = 0, \quad \forall l, m \in \mathbb{Z}, l \neq m, \tag{5.6}$$

the scaling relation (5.3) implies that

$$\sum_{k=0}^{2N-1} a_k a_{k-2m} = 0, \qquad \forall m \in \mathbb{Z}, m \neq 0 \tag{5.7}$$

(in (5.7), we take $a_{k-2m} = 0$ if $k - 2m \notin \{0, 1, ..., 2N-1\}$).

If relations (5.5) and (5.7) are satisfied the functions φ_{jl} defined by

$$\varphi_{jl}(x) = 2^{j/2}\varphi(2^j x - l) \tag{5.8}$$

(i.e., obtained from φ by *translation* and *dilation*) form a basis of $L^2(\mathbb{R})$.

The fact that the set $\{a_k\}_{k=0}^{2N-1}$ is *finite* implies that φ has a *compact support*. Without additional relations on the coefficients a_k, the scaling function φ *will not be smooth*, in general. Take, for example, $N = 1$ and $a_0 = a_1 = 1$, then the function φ defined by

$$\varphi(x) = 1 \quad \text{if} \quad 0 \leqslant x \leqslant 1, \qquad \varphi(x) = 0 \text{ elsewhere}$$

clearly satisfies (5.3)–(5.7); however, it is definitely a *discontinuous function*.

To force the smoothness of φ, we may require, for example, that the monomials $1, x, ..., x^{N-1}$ have to be *linear combinations* of the translates $\varphi(x-l)$; this will imply

$$\sum_{k=0}^{2N-1} (-1)^k k^m a_k = 0, \qquad \text{for} \quad m = 0, 1, ..., N-1. \tag{5.9}$$

Suppose that we have constructed a set $\{a_k\}_{k=0}^{2N-1}$ satisfying (5.5), (5.7), (5.9); to construct the scaling function φ from this set we may proceed as follows:

Taking the Fourier transform of both sides of (5.3) we obtain

$$\begin{aligned}\hat{\varphi}(s) &= \int_{\mathbb{R}} \varphi(x)\, e^{-2i\pi sx}\, dx \\ &= \hat{\varphi}\left(\frac{s}{2}\right)\left(\frac{1}{2}\sum_{k=0}^{2N-1} a_k e^{-i\pi sk}\right).\end{aligned} \tag{5.10}$$

Define the function P by

$$P(s) = \tfrac{1}{2}\sum_{k=0}^{2N-1} a_k e^{-2i\pi sk};$$

it follows then from (5.10) that we have

$$\hat{\varphi}(s) = \hat{\varphi}\left(\frac{s}{2}\right) P\left(\frac{s}{2}\right). \tag{5.11}$$

Reiterating (5.11)—and observing that (5.4) implies that $\hat{\varphi}(0) = 1$—we obtain the following *infinite product* relation

$$\hat{\varphi}(s) = \prod_{j=1}^{+\infty} P(2^{-j}s). \tag{5.12}$$

The scaling function φ is given then by

$$\varphi(x) = \int_{\mathbb{R}} \hat{\varphi}(s)\, e^{2i\pi sx}\, ds. \tag{5.13}$$

The *fast Fourier transform* can be used to obtain φ from $\hat{\varphi}$ in (5.13); actually, since it can be shown that the support of φ is the interval $[0, 2N-1]$, it suffices to know φ at $x = 0, 1, ..., 2N-1$, to obtain—via the scaling relation (5.3)—its values at any *dyadic number* of the interval $[0, 2N-1]$ (i.e., at any x of the above interval which has a *finite binary expansion*; we recall that the set of the dyadic real numbers is *dense* in $\mathbb{R}$).

The construction of the scaling function given here is the one discussed in [31]; see, e.g., [33] for other methods to construct φ.

The *basic wavelet function* ψ is defined from the coefficients a_k and from φ by

$$\varphi(x) = \sum_{k=2-2N}^{1} (-1)^k\, a_{1-k}\varphi(2x-k); \tag{5.14}$$

next, we define ψ_{jl} by

$$\psi_{jl}(x) = 2^{j/2}\psi(2^j x - l). \tag{5.15}$$

In order to use *wavelet based Galerkin solution methods*, we introduce for *n fixed* the following subspaces V_n and W_n of $L^2(\mathbb{R})$:

$$V_n = \text{closure of the linear space spanned by } \{\varphi_{nl}\}_{l \in \mathbb{Z}}, \tag{5.16}$$

$$W_n = \text{closure of the linear space spanned by } \{\psi_{nl}\}_{l \in \mathbb{Z}}. \tag{5.17}$$

Then the following properties hold:

$$V_n \subset V_{n+1}, \quad \forall n, \tag{5.18}$$

$$\text{closure}\left(\bigcup_n V_n\right) = L^2(\mathbb{R}), \tag{5.19}$$

$\{\varphi_{nl}\}_{l\in\mathbb{Z}}$ is an orthogonal basis for V_n, $\forall n$, (5.20)

W_n is the orthogonal complement of V_n in V_{n+1}, (5.21)

$\{\psi_{nl}\}_{l\in\mathbb{Z}}$ is an orthogonal basis for W_n, $\forall n$, (5.22)

φ_{nl} and ψ_{nl} have a compact support, $\forall n, l$, (5.23)

$$\int_{\mathbb{R}} \varphi_{nl}(x)\,dx = 2^{-n/2}, \qquad \int_{\mathbb{R}} \psi_{nl}(x)\,dx = 0, \quad \forall n, l. \tag{5.24}$$

A further consequence of (5.18)–(5.21) is

$$L^2(\mathbb{R}) = V_n \oplus \sum_{j\geq n} \oplus W_j, \qquad \forall n, \tag{5.25}$$

which clearly implies $L^2(\mathbb{R}) = V_0 \oplus \sum_{j\geq 0} \oplus W_j$.

Incidently, relation (5.25) is of fundamental importance to implement *wavelet based multilevel solution methods.*

The approximation properties of the Daubechies functions are discussed in, e.g., [30, 31]; observing that for N sufficiently large (see [30, 31] for a more precise statement) we shall have φ and ψ belonging to $H^m(\mathbb{R})$ (with $m < N$), it has been shown that if the function f is *sufficiently smooth* then

$$\|f - P_n(f)\|_{H^m(\mathbb{R})} = O(2^{-n(N-m)}),$$

where $P_n: L^2(\mathbb{R}) \to V_n$ is the *orthogonal projector* from $L^2(\mathbb{R})$ to V_n.

We have shown on Fig. 5.1 the graphs of the scaling function φ and wavelet function ψ, respectively, corresponding to $N = 3$.

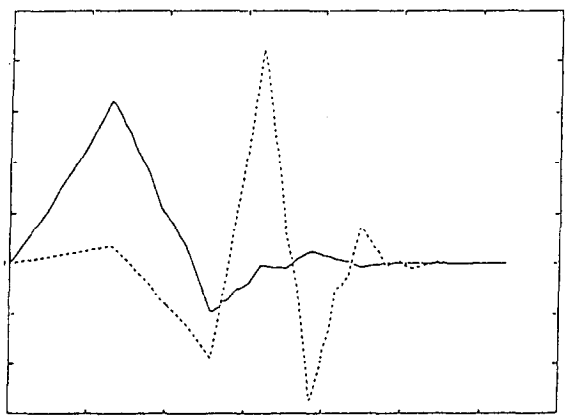

FIG. 5.1. Variation of φ(—) and ψ(⋯) if $N = 3$.

5.3. Application to the Solution of the Incompressible Navier–Stokes Equations

5.3.1. *Generalities*

The Navier–Stokes equations that we consider are those given by (5.1), (5.2), completed by initial and boundary conditions. Concerning the *wavelet* solution of the above Navier–Stokes equations, we see immediately three sources of potential difficulties, namely:

(i) The treatment of the *incompressibility condition* $\nabla \cdot \mathbf{u} = 0$.

(ii) The treatment of the *boundary conditions.*

(iii) The simulation of flow at large Reynolds numbers.

In this article we shall focus on (i); however, the two other issues deserve some comments:

Concerning *boundary conditions*, the *periodic case* is quite easy to implement; on the other hand, other boundary conditions such as Dirichlet and Neumann yield serious difficulties, the main reasons being that in a wavelet expansion the coefficients are not *pointwise* values of the function or of its derivatives, as is the case with finite elements or finite differences. Among the possible cures let us mention *boundary fitted wavelets* like the ones developed by S. Jaffard and Y. Meyer in [34], or *fictitious domain methods*, in the spirit of [35, 36]; we are currently investigating the second approach. Another possibility is to couple wavelet approximations (used away from the boundary) with finite elements (used in the neighborhood of the boundary), but the matching problems (at least for nonoverlapping couplings) are essentially as difficult to implement as are boundary conditions.

Concerning now the simulation of flow at large Reynold numbers we can predict, on the basis of preliminary numerical experiments done with the Daubechies wavelets, that for an equivalent amount of computational work, wavelet based methods *are more stable and accurate than finite element, finite difference, and spectral methods*, at least for problems with very simple geometry and boundary conditions. The above experiments involved the solution of the *Burgers equation* $u_t + uu_x = vu_{xx}$ (cf. [31, 32]) and of the *Navier–Stokes equations* with *periodic boundary conditions* (cf. [37]). A key property of wavelet based solution methods is that they seem to require much less (if any at all) artificial viscosity for highly advective flow; a possible explanation of this behavior is that it is a consequence of the orthogonality of the basis functions and of their localization properties in the spatial *and* spectral domains.

The treatment of the incompressibility seems to be eventually fairly simple and will be addressed in the next section.

5.3.2. *Wavelet Treatment of the Incompressibility Condition*

Operator splitting techniques applied to the solution of the Navier–Stokes equations (5.1), (5.2) lead to the following Stokes equations

$$\alpha \mathbf{u} - \nu \nabla^2 \mathbf{u} + \nabla p = \mathbf{f} \quad \text{in } \Omega, \tag{5.26}$$

$$\nabla \cdot \mathbf{u} = 0 \quad \text{in } \Omega. \tag{5.27}$$

We suppose that the boundary conditions are defined by

$$\mathbf{u} = \mathbf{g} \quad \text{on } \Gamma \quad \left(\text{with } \int_\Gamma \mathbf{g} \cdot \mathbf{n}\, d\Gamma = 0\right); \tag{5.28}$$

i.e., they are of the *Dirichlet* type.

A *variational formulation* of problem (5.26), (5.27) is given by

$$\mathbf{u} \in V_{\mathbf{g}}; \quad \forall \mathbf{v} \in V_0 \text{ we have}$$

$$\int_\Omega (\alpha \mathbf{u} \cdot \mathbf{v} + \nu \nabla \mathbf{u} \cdot \nabla \mathbf{v})\, dx \tag{5.29}$$

$$-\int_\Omega p \nabla \cdot \mathbf{v}\, dx = \int_\Omega \mathbf{f} \cdot \mathbf{v}\, dx,$$

$$\int_\Omega q \nabla \cdot \mathbf{u}\, dx = 0, \quad \forall q \in L^2(\Omega);\ p \in L^2(\Omega). \tag{5.30}$$

In (5.29), (5.30), we have $\mathbf{v} \cdot \mathbf{w} = \sum_{i=1}^d v_i w_i$, $\forall \mathbf{v} = \{v_i\}_{i=1}^d$, $\mathbf{w} = \{w_i\}_{i=1}^d$; $\nabla \mathbf{v} \cdot \nabla \mathbf{w} = \sum_{i=1}^d \sum_{i=1}^d (\partial v_i / \partial x_j)(\partial w_i / \partial x_j)$; $V_0 = (H_0^1(\Omega))^d$ and $V_g = \{\mathbf{v} \mid \mathbf{v} \in (H^1(\Omega))^d,\ \mathbf{v} = \mathbf{g} \text{ on } \Gamma\}$.

It follows from (5.29), (5.30) that the two fundamental spaces in the variational formulation of (5.26), (5.27) are $L^2(\Omega)$ (for the pressure) and $(H^1(\Omega))^d$ (for the velocity). We discuss now the wavelet approximation of the *variational problem* (5.29), (5.30):

From now on we shall denote by φ^N the *scaling function* associated to the positive integer N (the precise definition of the scaling function has been given in Section 5.2); the parameter N plays clearly the role of a polynomial degree. We define next φ_{jl}^N and $\Phi_n^N(\mathbb{R})$ by

$$\varphi_{jl}^N(x) = 2^{j/2} \varphi^N(2^j x - l), \quad \forall x \in \mathbb{R}, \tag{5.31}$$

$\Phi_n^N(\mathbb{R}) =$ closure of the linear space spanned by

$$\{\varphi_{nl}^N\}_{l \in \mathbb{Z}}, \tag{5.32}$$

respectively.

In order to apply wavelets to the solution of *multidimensional* problems an obvious approach is to use *tensor products* of one variable function spaces to define the multidimensional ones. We define therefore the spaces $\mathcal{W}_n^N(\mathbb{R}^d)$ and $V_n^N(\mathbb{R}^d)$ by

$$\mathcal{W}_n^N(\mathbb{R}^d) = \bigotimes_{i=1}^d \Phi_n^N(\mathbb{R}_{x_i}), \tag{5.33}$$

$$V_n^N(\mathbb{R}^d) = (\mathcal{W}_n^N(\mathbb{R}^d))^d, \tag{5.34}$$

respectively.

By restricting to Ω the elements of the two above spaces, we obtain $\mathcal{W}_n^N(\Omega)$ and $V_n^N(\Omega)$; if Ω is bounded, these two spaces are *finite dimensional*. On the basis of the analysis done in Section 2.4, concerning the finite difference and finite element approximations of the Stokes/Dirichlet problem (5.26)–(5.28) we shall approximate the *velocity spaces* V_0 and V_g by appropriate subspaces of $V_n^N(\Omega)$ (taking into account, in some way or another, the boundary conditions $\mathbf{v} = \mathbf{0}$ and $\mathbf{v} = \mathbf{g}$, respectively), and then the *pressure* space by $\mathcal{W}_{n-1}^N(\Omega)$; in order to have $V_n^N(\Omega) \subset H^1(\Omega)$, we have to take $N \geqslant 3$ (cf., e.g., [30, 31] for this result). We then substitute to V_0, V_g, and $L^2(\Omega)$, their wavelet analogues in (5.29), (5.30) to obtain a wavelet/Galerkin approximation of the Stokes problem (5.26)–(5.28).

The wavelet implementation of Dirichlet boundary conditions, for multidimensional problems (by *fictitious domain methods*, in particular), is presently under investigation.

APPENDIX: CONJUGATE GRADIENT SOLUTION OF THE STOKES PROBLEM

As announced in Section 2.5 we shall discuss in this appendix the preconditioned gradient solution of the *generalized Stokes problem*:

$$\alpha \mathbf{u} - \nu \nabla^2 \mathbf{u} + \nabla p = \mathbf{f} \quad \text{in } \Omega, \tag{A.1}$$

$$\nabla \cdot \mathbf{u} = 0 \quad \text{in } \Omega, \tag{A.2}$$

$$\mathbf{u} = \mathbf{g}_0 \quad \text{on } \Gamma_0, \qquad \nu \frac{\partial \mathbf{u}}{\partial n} - \mathbf{n} p = \mathbf{g}_1 \quad \text{on } \Gamma_1, \tag{A.3}$$

where $\Omega \subset \mathbb{R}^d$ $(d \geqslant 2)$ and where Γ_0, Γ_1 are two subsets of the boundary Γ of Ω, such that

$$\Gamma_0 \cap \Gamma_1 = \varnothing, \quad \text{closure}(\Gamma_0 \cup \Gamma_1) = \Gamma; \tag{A.4}$$

if $\Gamma_1 = \varnothing$ (i.e., $\Gamma = \Gamma_0$) we have to assume that

$$\int_\Gamma \mathbf{g}_0 \cdot \mathbf{n}\, d\Gamma = 0. \tag{A.5}$$

Following Section 2.3, we should easily prove that the *pressure* solution in (A.1)–(A.3) is the solution of

$$Ap = -\nabla \cdot \mathbf{u}_0, \tag{A.6}$$

where $\mathbf{u}_0$ is the solution of the elliptic system

$$\alpha \mathbf{u}_0 - \nu \Delta \mathbf{u}_0 = \mathbf{f} \quad \text{in } \Omega, \tag{A.7}$$

$$\mathbf{u}_0 = \mathbf{g}_0 \quad \text{on } \Gamma_0, \qquad \nu \frac{\partial \mathbf{u}_0}{\partial n} = \mathbf{g}_1 \quad \text{on } \Gamma_1, \tag{A.8}$$

and where operator A is defined by

$$Aq = \nabla \cdot \mathbf{u}_q, \qquad \forall q \in L^2(\Omega), \tag{A.9}$$

with $\mathbf{u}_q$ the solution of the following elliptic system:

$$\alpha \mathbf{u}_q - \nu \Delta \mathbf{u}_q = -\nabla q \quad \text{in } \Omega, \tag{A.10}$$

$$\mathbf{u}_q = 0 \quad \text{on } \Gamma_0, \qquad \nu \frac{\partial \mathbf{u}_q}{\partial n} = q\mathbf{n} \quad \text{on } \Gamma_1. \tag{A.11}$$

Using integration by parts we can easily prove that

$$\int_\Omega (Aq)\, q'\, dx = \int_\Omega (\alpha \mathbf{u}_q \cdot \mathbf{u}_{q'} + \nu \nabla \mathbf{u}_q \cdot \nabla \mathbf{u}_{q'})\, dx, \qquad \forall q, q' \in L^2(\Omega). \tag{A.12}$$

It follows from (A.12) that operator A is *symmetric* and—at least—positive semi-definite; indeed we have more since we also have

$$\int_\Omega (Aq) q\, dx \geqslant \gamma \, \|q\|^2_{L^2(\Omega)}, \qquad \forall q \in P, \tag{A.13}$$

where, in (A.13), γ is a *positive constant* and space P is defined by

$$P = L^2(\Omega), \qquad \text{if} \quad \Gamma_1 \neq \varnothing \tag{A.14}$$

and

$$P = \left\{ q \mid q \in L^2(\Omega), \int_\Omega q\, dx = 0 \right\}, \qquad \text{if} \quad \Gamma_0 = \Gamma. \tag{A.15}$$

From these properties, operator A is an isomorphism from P onto P, implying in turn that Eq. (A.6) has a *unique solution* in P, if the right-hand side $-\nabla \cdot \mathbf{u}_0$ belongs to P. If $\Gamma_1 \neq \varnothing$, it is clearly the case; if $\Gamma_0 = \Gamma$, we have

$$\int_\Omega \nabla \cdot \mathbf{u}_0\, dx = \int_\Gamma \mathbf{u}_0 \cdot \mathbf{n}\, d\Gamma = \int_\Gamma \mathbf{g}_0 \cdot \mathbf{n}\, d\Gamma = 0,$$

which implies that $-\nabla \cdot \mathbf{u}_0$ belongs to P and therefore that (A.6) has a unique solution.

Observe now that Eq. (A.6) is equivalent to the *linear variational problem*

$$p \in P, \qquad \int_\Omega (Ap) q\, dx = -\int_\Omega \nabla \cdot \mathbf{u}_0 q\, dx, \qquad \forall q \in P; \tag{A.16}$$

from the properties of operator A mentioned above, it appears that problem (A.16) is a particular case of those problems (P), whose solution has been discussed in Section 3.5.1. Problem (A.16) can be solved therefore by the conjugate gradient algorithm (3.18)–(3.25).

The corresponding algorithm will be fully defined once one has specified the scalar product to be used over space P. As discussed in [20, 38], the usual scalar product of $L^2(\Omega)$, namely,

$$\{q, q'\} \to \int_\Omega qq'\, dx,$$

leads to an algorithm with poor convergence properties if $\nu/\alpha \ll 1$. In order to have an algorithm performing well for *all* values of ν/α the following scalar product is advocated (and justified) in [20, 38],

$$\{q, q'\} \to \int_\Omega (S^{-1}q)\, q'\, dx,$$

where operator S: $P \to P$ is defined as

$$Sq = \nu q + \alpha \varphi_q, \qquad \forall q \in P, \tag{A.17}$$

with φ_q the solution of

$$-\Delta \varphi_q = q \quad \text{in } \Omega, \qquad \frac{\partial \varphi_q}{\partial n} = 0 \quad \text{on } \Gamma_0, \qquad \varphi_q = 0 \quad \text{on } \Gamma_1, \qquad \text{if} \quad \Gamma_1 \neq \varnothing, \tag{A.18}_1$$

$$-\Delta \varphi_q = q \quad \text{in } \Omega, \qquad \frac{\partial \varphi_q}{\partial n} = 0 \quad \text{on } \Gamma_0, \qquad \int_\Omega \varphi_q\, dx = 0, \qquad \text{if} \quad \Gamma_0 = \Gamma. \tag{A.18}_2$$

From a practical point of view *it is more important to know* S^{-1} *than* S to implement a conjugate gradient algorithm preconditioned by S.

The space P being equipped with the scalar product associated to S^{-1}, and, assuming that $\Gamma_1 \neq \varnothing$, algorithm (3.18)–(3.25) applied to the solution of problem (A.16) leads to the following algorithm (cf. also [38, Section 4.3.3]).

DESCRIPTION OF THE ALGORITHM.

$$p^0 \in P \text{ is given;} \tag{A.19}$$

solve

$$\begin{aligned} \alpha \mathbf{u}^0 - \nu \Delta \mathbf{u}^0 &= \mathbf{f} - \nabla p^0 \quad \text{in } \Omega, \\ \mathbf{u}^0 &= \mathbf{g}_0 \quad \text{on } \Gamma_0, \\ \nu \frac{\partial \mathbf{u}^0}{\partial n} &= \mathbf{g}_1 + \mathbf{n} p^0 \quad \text{on } \Gamma_1, \end{aligned} \tag{A.20}$$

and set

$$r^0 = \nabla \cdot \mathbf{u}^0. \tag{A.21}$$

Solve now

$$\begin{aligned} -\Delta \varphi^0 &= r^0 \quad \text{in } \Omega, \\ \frac{\partial \varphi^0}{\partial n} &= 0 \quad \text{on } \Gamma_0, \\ \varphi^0 &= 0 \quad \text{on } \Gamma_1, \end{aligned} \tag{A.22}$$

and set

$$g^0 = \nu r^0 + \alpha \varphi^0, \tag{A.23}$$

$$w^0 = g^0. \tag{A.24}$$

Then for $m \geq 0$, assuming that p^m, $\mathbf{u}^m$, r^m, g^m, w^m are known, compute p^{m+1}, $\mathbf{u}^{m+1}$, r^{m+1}, g^{m+1}, w^{m+1} as follows:
Solve

$$\begin{aligned} \alpha \bar{\mathbf{u}}^m - \nu \Delta \bar{\mathbf{u}}^m &= -\nabla w^m \quad \text{in } \Omega, \\ \bar{\mathbf{u}}^m &= \mathbf{0} \quad \text{on } \Gamma_0, \\ \nu \frac{\partial \bar{\mathbf{u}}^m}{\partial n} &= \mathbf{n} w^m \quad \text{on } \Gamma_1, \end{aligned} \tag{A.25}$$

and set

$$\bar{r}^m = \nabla \cdot \bar{\mathbf{u}}^m. \tag{A.26}$$

Compute

$$\rho_m = \frac{\int_\Omega r^m g^m \, dx}{\int_\Omega \bar{r}^m w^m \, dx}, \tag{A.27}$$

and then

$$p^{m+1} = p^m - \rho_m w^m, \tag{A.28}$$

$$\mathbf{u}^{m+1} = \mathbf{u}^m - \rho_m \bar{\mathbf{u}}^m, \tag{A.29}$$

$$r^{m+1} = r^m - \rho_m \bar{r}^m. \tag{A.30}$$

Solve, next,

$$\begin{aligned} -\Delta \bar{\varphi}^m &= \bar{r}^m \quad \text{in } \Omega, \\ \frac{\partial \bar{\varphi}^m}{\partial n} &= 0 \quad \text{on } \Gamma_0, \\ \bar{\varphi}^m &= 0 \quad \text{on } \Gamma_1, \end{aligned} \tag{A.31}$$

and compute

$$g^{m+1} = g^m - \rho_m (\nu \bar{r}^m + \alpha \bar{\varphi}^m). \tag{A.32}$$

If $\int_\Omega r^{m+1} g^{m+1} \, dx / \int_\Omega r^0 g^0 \, dx \leq \varepsilon$, take $p = p^{m+1}$, $\mathbf{u} = \mathbf{u}^{m+1}$; if not compute

$$\gamma_m = \int_\Omega r^{m+1} g^{m+1} \, dx \Big/ \int_\Omega r^m g^m \, dx, \tag{A.33}$$

and then

$$w^{m+1} = g^{m+1} + \gamma_m w^m. \tag{A.34}$$

Do $m = m + 1$ and go back to (A.25).

Algorithm (A.19)–(A.34) has proved to be quite efficient for solving Navier–Stokes equations on a quite large range of Reynolds number. To conclude this Appendix we have the following remarks:

Remark A.1. In the case where $\Gamma_0 = \Gamma$, we should replace (A.20), (A.22), (A.25), (A.31) by

$$\begin{aligned} \alpha \mathbf{u}^0 - \nu \Delta \mathbf{u}^0 &= \mathbf{f} - \nabla p^0 \quad \text{in } \Omega, \\ \mathbf{u}^0 &= \mathbf{g}_0 \quad \text{on } \Gamma, \end{aligned} \tag{A.20}'$$

$$\begin{aligned} -\Delta \varphi^0 &= r^0 \quad \text{in } \Omega, \\ \frac{\partial \varphi^0}{\partial n} &= 0 \quad \text{on } \Gamma, \quad \int_\Omega \varphi^0 \, dx = 0, \end{aligned} \tag{A.22}'$$

$$\begin{aligned} \alpha \bar{\mathbf{u}}^m - \nu \Delta \bar{\mathbf{u}}^m &= -\nabla w^m \quad \text{in } \Omega, \\ \bar{\mathbf{u}}^m &= \mathbf{0} \quad \text{on } \Gamma, \end{aligned} \tag{A.25}'$$

$$\begin{aligned} -\Delta \bar{\varphi}^m &= \bar{r}^m \quad \text{in } \Omega, \\ \frac{\partial \bar{\varphi}^m}{\partial n} &= 0 \quad \text{on } \Gamma, \quad \int_\Omega \bar{\varphi}^m \, dx = 0, \end{aligned} \tag{A.31}'$$

respectively.

Remark A.2. Taking $\varepsilon = 10^{-14}$ in the above stopping criterion has provided very satisfactory results when running on the CRAY X-MP.

Remark A.3. In practice one solves a finite dimensional analogue of problem (A.16), obtained by a finite difference, or finite element, or spectral approximation of the Navier–Stokes equations (see, e.g., [38, Sections 4 and 5] for this aspect of the solution process).

ACKNOWLEDGMENTS

The author would like to acknowledge the help of the following individuals for friendly discussions and/or collaboration: A. Bensoussan, J. P. Benque, M. O. Bristeau, J. Cahouet, J. P. Chabard, E. J. Dean, L. Franca, J. Goussebaile, A. Haugel, C. H. Li, G. Labadie, I. Lasiecka, W. Lawton, J. L. Lions, J. Periaux, O. Pironneau, H. Resnikoff, D. L. Russel, R. Triggiani, J. Weiss, R. O. Wells. He acknowledges also the helpful comments and suggestions from Dr. P. L. Roe and from the reviewers. The support of the following corporations or institutions is also acknowledged: AWARE, CRAY Research, Dassault Industries, EDF, INRIA, LCC-Rio de Janeiro, University of Colorado, University of Houston, Université Pierre et Marie Curie. We also benefited from the support of DARPA (Contracts AFOSR F49620-89-C-0125 and AFOSR-90-0334) and NSF (Grant INT 8612680). Finally, special thanks are due to the Editors of the *Journal of Computational Physics* for suggesting us to write an invited article, and to J. A. Wilson for diligently processing a preliminary version of it.

REFERENCES

1. R. Glowinski, P. Le Tallec, M. Ravachol, and V. Tsikkinis, in *Finite Elements in Fluids, Volume* 8, edited by T. J. Chung (Hemisphere Publishing Corporation, Washington, 1992), p. 137.
2. P. F. Fisher, L. W Ho, G. G. Karniadakis, E. M. Ronquist, and A. T. Patera, *Comput. Struct.* **30**, 217 (1988).
3. R. Glowinski, C. H. Li, and J. L. Lions, *Jpn J. Appl. Math.* **7**, 1 (1990).
4. E. J. Dean, R. Glowinski, and C. H. Li, *Comput. Phys. Commun.* **53**, 401 (1989).
5. J. L. Lions, *C.R. Acad. Sci. Paris Sér. I* **302**, 471 (1986).
6. J. L. Lions, *SIAM Rev.* **30**, 1 (1988).
7. J. L. Lions, *Controlabilité Exacte, Perturbation et Stabilisation des Systèmes Distribués* (Masson, Paris, 1988), Vols. 1 and 2.
8. R. A. Adams, *Sobolev Spaces* (Academic Press, New York, 1975).
9. J. Necas, *Les Méthodes Directes en Théorie des Equations Elliptiques* (Masson, Paris, 1967).
10. R. Glowinski and P. Le Tallec, *Augmented Lagrangian and Operator-Splitting Methods in Nonlinear Mechanics* (SIAM, Philadelphia, 1989).
11. C. Bernardi, C. Canuto, and Y. Maday, *SIAM J. Num. Anal.* **25**, 1237 (1988).
12. C. Bernardi and Y. Maday, *Int. J. Numer. Methods Fluids* **8**, 537 (1988).
13. V. Girault and P. A. Raviart, *Finite Element Approximation of the Navier–Stokes Equations* (Springer-Verlag, Berlin, 1986).
14. E. Thomasset, *Implementation of Finite Element Methods for Navier–Stokes Equations* (Springer-Verlag, New York, 1981).
15. M. O. Bristeau, R. Glowinski, and J. Periaux, *Comput. Phys. Rep.* **6**, 73 (1987).
16. M. Gunzberger, *Finite Element Methods for Viscous Incompressible Flows* (Academic Press, Boston, 1989).
17. O. Pironneau, *Finite Element Methods for Fluids* (Wiley, Chichester, 1989).
18. R. Glowinski, *Numerical Methods for Nonlinear Variational Problems* (Springer-Verlag, New York, 1984).
19. T. J. R. Hughes, L. P. Franca, and M. Balestra, *Comput. Methods Appl. Mech. Eng.* **59**, 85 (1986).
20. J. Cahouet and J. P. Chabard, *Int. J. Numer. Methods Fluids* **8**, 269 (1988).
21. R. Glowinski and C. H. Li, *C.R. Acad. Sci. Paris, Sér. I* **311**, 135 (1990).
22. D. L. Russel, *SIAM Rev.* **20**, 639 (1978).
23. W. Littman, *Ann. Scuola Norm. Sup Pisa* **4**, 567 (1978).
24. J. L. Lions, private communication (1988).
25. A. Bensoussan, *Acta Appl. Math.* **20**, 197 (1990).
26. J. Daniel, *The Approximate Minimization of Functionals* (Prentice–Hall, Englewood Cliffs, NJ, 1970).
27. P. A. Raviart and J. M. Thomas, in *Energy Methods in Finite Element Analysis*, edited by R. Glowinski, E. Y. Rodin, and O. C. Zienkiewicz (Wiley, Chichester, 1979), p. 175.
28. R. Glowinski, W. Kinton, and M. F. Wheeler, *Int. J. Numer. Methods Eng.* **27**, 623 (1989).
29. R. Glowinski, C. H. Li, and J. L. Lions, in preparation.
30. I. Daubechies, *Commun. Pure Appl. Math.* **41**, 909 (1988).
31. R. Glowinski, W. Lawton, M. Ravachol, and E. Tenenbaum, in *Computing Methods in Applied Sciences and Engineering*, edited by R. Glowinski and A. Lichnewsky (SIAM, Philadelphia, 1990), p. 55.
32. A. Latto and E. Tenenbaum, *C.R. Acad. Sci. Paris, Sér. I* **311**, 903 (1990).
33. G. Strang, *SIAM Rev.* **31**, 614 (1989).
34. S. Jaffard and Y. Meyer, *J. Math. Pures Appl.* **68**, 95 (1989).
35. C. Borgers, *Numer. Math.* **57**, 435 (1990).
36. D. P. Young, R. G. Melvin, M. B. Bieterman, F. T. Johnson, S. S. Samant, and J. E. Bussoletti, *J. Comput. Phys.* **92**, 1 (1991).
37. J. Weiss, Wavelets and the study of two-dimensional turbulence, AWARE Report, 1991 (unpublished).
38. R. Glowinski, in *Vortex Dynamics and Vortex Methods*, edited by C. R. Anderson and C. Greengards (Am. Math. Soc., Providence, RI, 1991), p. 219.